Supporting Information for

Acetolysis of waste PET for upcycling and life-cycle assessment study

Yuantao Peng[1], Jie Yang[1], Chenqiang Deng[1], Yao Fu[1]* and Jin Deng[1]*

[1]CAS Key Laboratory of Urban Pollutant Conversion, Anhui Province Key Laboratory of Biomass Clean Energy Department of Applied Chemistry, University of Science and Technology of China, Hefei, Anhui, 230026, PR China

*Corresponding author. E-mail: dengjin@ustc.edu.cn

This supplementary information file includes:

1. Supplementary Notes 1-4.
2. Supplementary Tables S1-S19
3. Supplementary Figures S1-S27
4. Supplementary video 1.
5. Supplementary Reference 1-17.

Supplementary Notes

Supplementary Note 1: The kinetics of PET degradation by acetolysis

PET hydrolysis has been previously reported to follow first-order kinetics[1-3]. Therefore, we assumed that the kinetics of acetolysis of PET was also the first-order kinetics, and its kinetic equation could be expressed as follows (1):

$$ln\frac{1}{1-y} = kt \qquad (1)$$

where y, *k*, and t are the depolymerization rate of PET (for simplicity, the yield of EGDA was used instead of the depolymerization rate of PET), the rate constant of the reaction, and the reaction time, respectively.

According to the depolymerization rate of PET at different temperatures (200 ºC, 220 ºC, 240 ºC, 260 ºC, 280 ºC) and different times, the rate constant *k* at different temperatures could be obtained by linear fitting, and then ***Ea*** of the reaction could be obtained from Arrhenius equation (2):

$$lnk = lnA - \frac{Ea}{RT} \qquad (2)$$

where k, A, R, and T are the rate constant of the reaction, the pre-exponential factor, the gas constant (8.31 J/k mol), and the absolute temperature in Kelvin, respectively.

The effect of reaction temperature on *k* calculated by equation (1) was shown in Fig. S1a. The experimental data showed a good linear relationship at different temperatures (Pearson's r > 0.98). In addition, the *k* value increases significantly with the increase of depolymerization temperature, which showed that temperature is the key factor affecting PET degradation. Fig. S1b was an Arrhenius plot of apparent *k* with good linear correlation (Pearson's r = 0.9985). Therefore, it was reasonable to assume that the acetolysis of PET follows the first-order kinetics. According to the slope of the Arrhenius curve, the apparent activation energy of the reaction was 127.38 kJ / mol, which was comparable to the ***Ea*** of other acid hydrolysis[4,5].

Supplementary Note 2: Process details and descriptions for Case 1 and Case 2 in ASPEN

In this simulation, poly-NRTL physical property method was selected to deal with PET depolymerization and polymerization process[6-9] (RBATCH1, CSTR1-2, RPLUG), At the same time, for other processes such as distillation, NRTL physical property method was used, in particular, when dealing with acetic acid aqueous solution system, NRTL-HOC physical property method is used to accurately simulate.

Case 1(Fig. S2): The discarded PET fragments were mixed with acetic acid and then enter the intermittent reaction kettle (RBATCH1). The depolymerization was carried out at 280 ℃ for 2 h. Then the reacted material was cooled (the heat from this process can produce high-pressure steam) and filtered to separate solid TPA. The liquid phase entered the rectification column (RADFRAC1) to further separate EGDA and HOAc. A small amount of PET oligomer remained in the liquid phase of the tower kettle (OLI-PET1) after depolymerization. Gaseous EGDA was extracted near the sideline of the bottom and a small amount of EGDA was separated from the oligomer by flash evaporation (FLASH1). The second section is EGDA hydrolysis, where the combined EGDA was mixed with a hydrochloric acid solution (HCl-H_2O) with a concentration of 0.2 M and then hydrolyzed in an intermittent reactor (RBATCH2) with hydrolysis kinetics data from Julio F. Mata-Segreda et al[10]. The hydrolysate was separated from the mixture of HCl, H_2O, HOAc and EG by a distillation

column (RADFRAC2), from strong to weak the order of volatility is HCl>H_2O>HOAc>EG. Compared with H_2O/HOAc, HOAc/EG has a greater volatility difference and is easier to separate. At the same time, to avoid subsequent re-esterification inversion, high-purity EG should be separated as far as possible in the presence of HCl. Therefore, it is selected to be separated from HOAc/EG here, HOAc is the light key component, and EG is the heavy key component. To save energy, the fraction at the top of the tower directly entered the next distillation column (RADFRAC3) without cooling. The high purity acetic acid (HOAC2) at the bottom of the tower (RADFRAC3) has a high recovery rate which can be returned to the first section for re-depolymerization of PET. Similarly, hydrochloric acid aqueous solution (RHCl-H_2O) at the top of the tower can also be recovered and returned to the second section for EGDA hydrolysis. The third section is re-polymerization, where high-purity EG was mixed with TPA and then esterified in an all-mixing reactor (CSTR1, CSTR2). After each reactor, residual EG was collected and separated from water in RADFRAC4 and returned to the aggregate. Finally, PET polyester with high molecular weight (PRO-PET) was obtained by high vacuum operation (280 ℃, 1 mmHg) in the post-polymerization reactor (RPLUG), the kinetic data of the polymerization process were obtained from Ref. 9.

Case 2 is very similar to Case 1 except for Section 2 (Fig. S2). Section 3 is a re-polymerization stage. Since there is no model for polymerization between EGDA and TPA, we estimated this process based on the dynamic data from the polymerization process between EG and TPA. At the same time, new polymer segments and oligomers are redefined (Tables S8).

Supplementary Note 3: Life-cycle assessment

The goal and scope of the LCA study in this work are shown in Table S9. Besides, the system boundary of LCA was set as "cradle to gate" (i.e. collection and transportation of waste PET; Production of chemical raw materials; And the whole process of post-depolymerization and re-polymerization to produce new PET) because the subsequent use and disposal of various PET products vary widely. Since there is no data on the pretreatment process of waste PET plastic collected in the early stage, we can only assume that it is consistent with the mechanical recycling[11]. At the same time, our distribution principle followed the “cut-off” rule that the first life cycle (original plastic) and the second life cycle (recycled plastic) are independent of each other. For inventory analysis, our material balance and energy balance were derived from actual experimental results and Aspen simulation results. These were our “prospective processes”, and the functional unit was set at 1 kg of new PET product. The impact assessment was carried out on professional software OpenLCA 1.10.3, and the assessment method was IMPACT 2002+. “Background process” data were obtained from database Ecoinvent V.3.7.1. The carbon footprint corresponding to electricity, steam, cooling water and chemical raw materials and their reference sources were detailed in Table S10-11. Herein, we mainly focused on non-renewable energy use (NREU, the result is expressed by MJ per kg PET) and Global Warming Potential (GWP, the result is expressed by kg CO_2 equivalent/kg PET, namely kg CO_2-eq per kg PET).

Supplementary Note 4: Kilogram scale degradation of post-consumer PET plastic waste through acetolysis

Reaction equation:

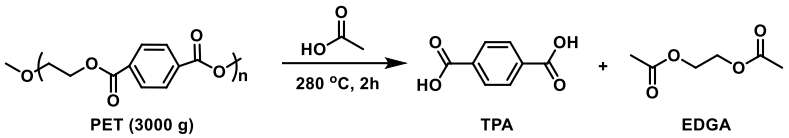

Reaction equipment: 20L Hastelloy-C276 mechanical stirring autoclave with sampling valve (working pressure range: 1-30 atm; working temperature range: r.t-350 °C)

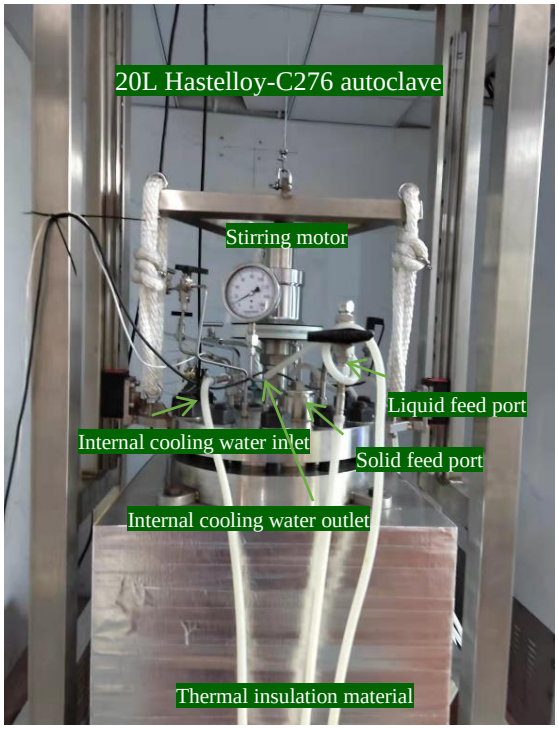

Input form: Post-consumer PET plastic waste: 3000 g (15.6 mol)
Glacial acetic acid (purity ≥99.5%): 15 L

Reaction conditions: Reaction temperature: 280 ºC (from room temperature to 280 ºC at 5 ºC/min)
Reaction time: 2 hours
Stirring rate: 60 rpm

Operation process: The weighed post-consumer PET plastic waste (3000 g) and glacial acetic acid (15 L) were put into the autoclave in turn. After sealing the autoclave, mechanical stirring was started and the speed was controlled at 60 rpm. The autoclave was heated to 280 ºC for two hours. After the reaction, the autoclave was cooled down to room temperature with internal cooling water. The reaction liquid and products were taken out through the valve at the bottom of the autoclave.

Post-processing:

Terephthalic acid was separated by suction filtration, then washed with water several times and dried in a drying oven. We finally obtained 2350g TPA with a yield of 90.60% (purity: 99.86%).

The acetic acid in the reaction solution was spun out under reduced pressure, and the vacuum degree was controlled at 15±5mmHg.

Then, the remaining liquid (2578g) was distilled under reduced pressure by an oil pump, the vacuum degree was controlled in the range of 2-4 mmHg, the fractions at different temperatures were collected, and analyzed by GC.

Fraction composition:

Fractions	Weight	HOAc	EGDA	Others
front cut fraction (≤ 60 °C)	240g	197.3g (82.2%)	41.5g (17.3%)	1.2g (0.5%)
main fraction (60 - 80 °C)	**2095g**	**35.6g (1.7%)**	**2057.3g (98.2%)**	**2.1g (0.1%)**
distillation residue	158g	0.8g (0.5%)	37.2g (23.5%)	120.0g (76.0%)
sum	2493g	233.7g (9.4%)	2136.0g (85.7%)	123.3g (4.9%)

Vacuum distillation loss: 2578g – 2493g = 85g

Yield of EGDA: 2136.0g / 2281.3g = 93.6%

Isolated yield of EGDA: 2057.3g / 2281.3g = 90.2% (purity: >98%)

			
Waste PET fragments	Glacial acetic acid	After reaction	Suction filtration
			
Remove acetic acid	Vacuum distillation	Solid product (TPA)	Liquid product (EGDA)

Supplementary Tables

Table S1. Effects of different organic acids on PET degradation through acetolysis.

Entry	Organic acids	TPA Yield/%	TPA Purity/%	EGDA Yield/%
1	Acetic acid	95.0 ± 1.2	99.83 ± 0.12	93.8 ± 1.6
2	Propionic acid	86.6 ± 1.2	99.51 ± 0.32	85.9 ± 1.8
3	*n*-Butyrate	88.0 ± 1.4	99.42 ± 0.32	86.2 ± 1.6
4	*n*-Valeric acid	87.1 ± 1.2	99.59 ± 0.28	86.3 ± 1.6
5	*n*-Caproic acid	86.8 ± 1.4	99.43 ± 0.28	84.2 ± 1.6

Reaction conditions: PET bottle fragments (60 g), organic acid (300 mL), reaction temperature (280 ºC), reaction time (2 h).

Table S2. Effect of reaction temperature on acetolysis of PET.

Entry	Temp./℃	Time/h	TPA Yield /%	TPA Purity/%	EDGA Yield/%
1	185	18	30.2 ± 1.4	70.2 ± 0.82	18.1 ± 2.4
2	200	18	72.6 ± 1.4	95.07 ± 0.78	68.5 ± 2.8
3	220	10	95.0 ± 1.6	99.43 ± 0.46	92.4 ± 2.6
4	250	8	93.8 ± 1.2	99.25 ± 0.42	91.3 ± 2.4
5	280	2	95.8 ± 1.4	99.72 ± 0.26	95.3 ± 2.4

Reactions conditions: PET bottle fragments (60 g), 300 mL acetic acid.

Table S3. Effect of waste plastic concentration on acetolysis of PET.

Entry	Concentration of PET*/(% w/v)	TPA Yield/%	TPA Purity/%	EDGA Yield/%
1	5	93.3 ± 2.2	99.33 ± 0.36	90.3 ± 2.0
2	10	95.0 ± 1.6	99.43 ± 0.40	89.8 ± 1.8
3	20	95.5 ± 1.2	99.50 ± 0.32	95.6 ± 1.6
4	50	78.2 ± 3.6	97.35 ± 0.42	68.8 ± 3.4
5	100	75.2 ± 4.2	97.09 ± 0.48	68.2 ± 3.8

Reactions conditions: PET bottle fragments (1.25 ~ 25 g), 25 mL acetic acid, 280 °C, 2 h.

* Concentration of PET = **[**mass of PET (g) / volume of acetic acid (mL)] × 100%

Table S4. Effect of water content on acetolysis of PET.

Entry	Water quality	TPA Yield/%	TPA Purity/%	EGA Yield/% (EGDA: EGMA)
1	-	95.2 ± 1.4	99.62 ± 0.36	95.5 (100%:0)
2	2% H2O	95.7 ± 1.4	99.63 ± 0.32	96.2(90%:10%)
3	5% H2O	96.1 ± 1.4	99.61 ± 0.34	96.5(79%: 21%)
4	10%H2O	92.3 ± 1.2	99.54 ± 0.30	87.1(64%: 36%)
5	20%H2O	89.4 ± 1.4	98.3 ± 0.52	83.6(40%: 60%)
6	40%H2O	70.2 ± 1.6	96.42 ± 0.50	63.3(18%: 82%)

Reactions conditions: PET bottle fragments (5.0 g), solvent (25 mL acetic acid or aqueous solution of acetic acid with different water content), 280 °C, 2 h.

Table S5. Acetolysis of waste PET from different sources

Category	Sources	TPA	TPA Yield/%	EGDA Yield/%
PET powder	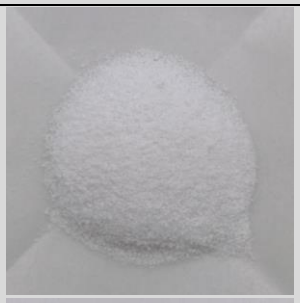		98.9 ± 1.0	98.3 ± 0.6
PET particle			97.7 ± 1.2	97.0 ± 0.8
Transparent bottle			96.2 ± 1.2	95.7 ± 0.8
Blue bottle			96.4 ± 1.0	95.6 ± 0.8
Green bottle			96.1 ± 1.6	95.2 ± 0.7
brown bottle			95.9 ± 1.4	95.1 ± 0.6

Black box			93.7 ± 1.4	93.3 ± 0.8
Black tray		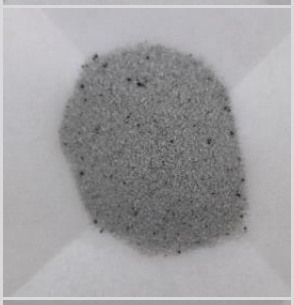	91.5 ± 1.8	91.0 ± 1.0
Transparent tray			95.5 ± 0.8	92.5 ± 0.6
Transparent box			96.5 ± 0.8	95.4 ± 0.6
PET+PE			94.1 ± 1.4	93.6 ± 0.6
PET/PP		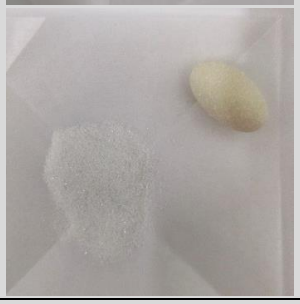	96.2 ± 1.4	95.6 ± 0.8

Reactions conditions: Waste plastic (60g), 300 mL acetic acid, 280 ºC, 2 h.

Table S6. Determine the content of 4-CBA and *p*-TOL in TPA by HPLC[12]

The source of TPA	4-CBA (mg/kg)	*p*-TOL (mg/kg)
TPA obtained from bottles.	n. d.	102.3
TPA obtained from textiles.	n. d.	127.3
TPA decolorized in an alkaline solution with activated carbon.	n. d.	118.5
TPA decolorized in N, N-dimethylacetamide with activated carbon.	n. d.	119.2
TPA decolorized in hot water (280°C) with activated carbon.	n. d.	108.6
The GB/T 32685-2016 standard[13]	≤25	≤150
The ASTM D7976-2020 International standard[14]	≤25	≤190

These decolorized TPA can be seen in Extended Data Fig.5. n. d. = not detected.

Table S7. Acetolysis of other plastics

	PETG	PEF	PEN	PBT
Polyester				
Structure	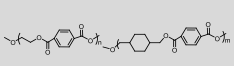	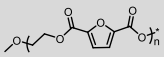	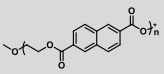	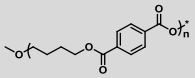
Product				
	TPA	2,5-FDCA	2,6-NDA	TPA
Yield/%	87.3 ± 1.8	89.3 ± 1.4	88.9 ± 2.4	92.3 ± 1.6

Reactions conditions: Waste plastic (5.0g), 25 mL acetic acid, 280 ºC, 2 h.

Table S8. Properties of the components not included in the Aspen database in Case 2

Compound	Heat of formation ($kJ \cdot kmol^{-1}$)	Density ($kg \cdot m^{-3}$)	Boiling points (℃)	Molecular weight ($g \cdot mol^{-1}$)
PET[15]	-485510	-	-	192.171
BAET[a]	-121527	1732.58	371.02	338.31
T-EGDA[b]	-	-	-	-

[a] BAET is the hypothesized intermediate during polymerization of the EGDA and TPA, it's estimated by the NIST ThermoData engine in Aspen.

[b] T-EGDA is the hypothetical terminal segment of polymer. It's estimated using Flory-Huggins theoretical calculation [16,17] in Aspen. The structural formula is as follows:

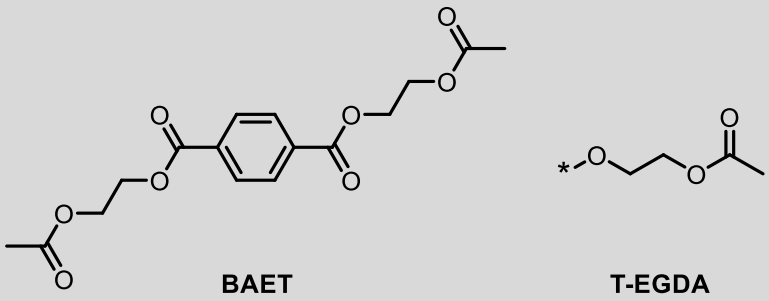

Table S9. Goal and scope definition of this LCA study	
Goal	
Reason for conducting the study	To evaluate the environmental impact of the acetic acid depolymerization process and compare it with other depolymerization processes in the literature
Audience	Industrial stakeholders, the research community and the public
Application	To further reduce carbon emissions from the recycling process of waste plastics
The intention of using results in a comparative study	Yes, the results are to be compared and disclosed to the public through this article publication
Scope	
Product system	The waste PET depolymerization section with the new PET production
Function	To depolymerize waste PET using acetic acid and produce new PET
Functional unit	1 kg of new PET
System boundary	See Fig. 1 in the next part
Allocation	In this study, additional raw materials such as acetic acid and hydrochloric acid aqueous solution have high recovery, so there are almost only electricity and high-pressure steam consumption in this system. As such, a simplified LCA model is developed where input and output data are allocated to the new PET produced.
Assumptions	(I) The pre-treatment discharge of waste PET is consistent with the mechanical method (II) This system deals with 12500 kg waste PET per hour over 8000 hours per year (III) This system is located in Europe
Requirements on data and quality	Material and energy consumption data were obtained from Aspen Plus and the background process was obtained from Ecoinvent V.3.7.1 in Open LCA 1.10.3.
LCIA methodology	IMPACT 2002+
Impact categories assessed in the study	(I) Global Warming Potential (100 years), kg CO_2 equivalent; (II) Non-renewable energy use, MJ;
Limitations	In addition to the above-mentioned assumptions, the following aspects are not assessed in this study: Plant construction and equipment maintenance.
Report requirements	To present the outcome via journal publication which is openly accessible to everyone.

Table S10. Carbon footprint values of each raw material of PET acetic acid hydrolysis process used in the Open LCA

Process	Value	Unit	Location
Acetic acid production	1.10386	kg $CO_{2\text{-eq}}$ per kg	Europe
Tap water production	0.00025	kg $CO_{2\text{-eq}}$ per kg	Europe without Switzerland
Electricity, high voltage, production mix	0.31260	kg $CO_{2\text{-eq}}$ per kwh	United Kingdom
Steam production, as an energy carrier, in the chemical industry	0.10040	kg $CO_{2\text{-eq}}$ per MJ	Europe

Table S11. Non-renewable energy use values of each raw material of PET acetic acid hydrolysis process used in the Open LCA

Process	Value	Unit	Location
Acetic acid production	46.86688	MJ per kg	Europe
Tap water production	0.00536	MJ per kg	Europe without Switzerland
Electricity, high voltage, production mix	8.73325	MJ per kwh	United Kingdom
Steam production, as an energy carrier, in the chemical industry	1.63695	MJ per MJ	Europe

Table S12. Energy balance of case 1

Equipment	RBATCH1	COOLER1	SEP	PUMP1	RADFRAC1		COOLER2	FLASH1	COOLER3	COOLER4
Cost/kw	-171.96	-9155.27	-2.49	0.34	CON: -6789.28	REB: 10350.00	-927.32	7.96	-9.56	-0.30

Table S12 continued

Equipment	RBATCH2	PUMP2	RADFRAC2		COMP1	RADFRAC3	
Cost/kw	5366.49	0.36	CON: -1174.39	REB:25308.60	267.96	CON: -53095.80	REB: 28745.00

Table S12 continued

Equipment	PUMP3	CSTR1	FLASH2	CSTR2	FLASH3	COMP2	RPLUG	FLASH4	RADFRAC4		M-COMP		COOLER
Cost/kw	2.92	5856.58	0	716.25	0	21.26	535.66	0	CON: -486.81	REB: 163.77	CON: -206.75	WORK: 213.48	-1211.98

Table S13. Utilitiy of case 1

Unit processes used	Type of Utility	Quantity	Function
COOLER1	U-2	12138.60 kg/h	Cool the product and co-produce steam for RADFRAC1
PUMP1	Electricity	0.34 kwh	Increase the pressure of the fluid
RADFRAC1	U-1; U-3	U-1:9432.90 kg/h; U-2:21671.20 kg/h	U-1: Cool the top fraction; U-3: Heat the tower kettle;
COOLER2	U-1	1288.20 kg/h	Cooling
FLAH1	U-3	16.70 kg/h	Heating
COOLER3	U-1	13.30 kg/h	Cooling
COOLER4	U-1	0.40 kg/h	Cooling
RBATCH2	Electricity	5366.50 kwh	Heating
PUMP2	Electricity	0.36 kwh	Increase the pressure of the fluid
RADFRAC2	U-1; U-3	U-1:1631.70 kg/h U-3:52992.30 kg/h	U-1: Cool the top fraction; U-3: Heat the tower kettle;
COMP1	Electricity	267.96 kwh	Increase the pressure of the fluid
RDAFRAC3	U-1; U-3	U-1:762700.00 kg/h; U-3:59682.60 kg/h	U-1: Cool the top fraction; U-3: Heat the tower kettle;
PUMP3	Electricity	2.92 kwh	Increase the pressure of the fluid
CSTR1	Electricity	5856.60 kwh	Heating
CSTR2	Electricity	716.30 kwh	Heating
RPLUG	Electricity	535.70 kwh	Heating
COMP2	Electricity	21.26 kwh	Increase the pressure of the fluid
RADFRAC4	U-1; U-3	U-1:6992.80 kg/h; U-3:302.80 kg/h	U-1: Cool the top fraction; U-3: Heat the tower kettle;
MCOMP	U-1; Electricity	U-1:287.30 kg/h Electricity:213.50 kwh	U-1: Compressor interstage cooling; Electricity: Increase the pressure
COOLER5	U-4	17409.60 kg/h	Cooling

Table S14. Details of the utilities of case 1

Type of utility used	Initial and final state of utility	
	Initial	Final
U-1	20 ℃; 1 atm; liquid phase	100 ℃; 1 atm; gaseous phase
U-2	20 ℃; 1 atm; liquid phase	250 ℃; 39.2 atm; gaseous phase
U-3	250 ℃; 39.2 atm; gaseous phase	249 ℃; 38.6 atm; liquid phase
U-4	20 ℃; 1 atm; liquid phase	80 ℃; 1 atm; liquid phase
Electricity	-	

Table 15. Mass balance of case 1

Para.	HOAC	WAS-PET	HOAC1	S2	PRODUCT	LIQUID1	TPA	LIQUID2	EGDA1	OLI-PET1	EGDA2	EGDA3	EGDA4	OLI-PET2	OLI-PET3
Temp./°C	25.00	25.00	118.23	280.00	30.10	30.00	30.00	30.00	215.90	215.90	188.45	224.69	190.133	224.69	35.00
Pres./kPa	101.33	101.33	102.00	3240.00	105.00	105.00	105.00	121.59	122.27	122.27	101.33	10.00	101.33	10.00	101.33
W-PET	0	12500.00	0	67.91	67.91	67.91	0	67.91	6.61E-22	67.91	6.61E-22	1.77E-76	1.77E-76	67.91	67.91
EGDA	0	0	18.29	9472.69	9472.69	9472.69	0	9472.69	9357.83	96.57	9357.83	94.00	94.00	2.56	2.56
TPA	0	0	0	10747.60	10747.60	0	10747.60	0	0	0	0	0	0	0	0
HOAC	7812.20	0	54511.60	54553.90	54553.90	54553.90	0	54553.90	42.17	0.076	42.17	0.075	0.075	0.00040	0.00040
H_2O	0	0	0	0	0	0	0	0	0	0	0	0	0	0	0
HCL	0	0	0	0	0	0	0	0	0	0	0	0	0	0	0
EG	0	0	0	0	0	0	0	0	0	0	0	0	0	0	0
PET	0	0	0	0	0	0	0	0	0	0	0	0	0	0	0
BHET	0	0	0	0	0	0	0	0	0	0	0	0	0	0	0

the unit in the material list is kg/h

Table S15 continued

Para.	EGDA5	HCL-H2O	S3	S4	S5	HOAC-H2O	EG	HGL	RHCL-H2O	HOAC2	S6	HS6	REG	S7
Temp./°C	188.46	25.00	42.24	85.00	90.59	103.55	203.53	103.96	88.78	123.93	98.93	99.26	203.48	260.00
Pres./kPa	101.33	101.33	101.33	101.33	121.59	101.33	121.59	111.46	101.33	121.59	105.00	810.60	121.59	810.60
W-PET	6.61E-22	0	6.61E-22	0	0	0	0	0	0	0	0	0	0	0
EGDA	9451.84	0	9451.84	2.22	2.22	0.0025	2.21	0.0025	1.47E-32	0.0025	2.21	2.21	9.21	11.42
TPA	0	0	0	0	0	0	0	0	0	0	10747.70	10747.70	15.67	1258.63
HOAC	42.24	0	42.24	7808.25	7808.25	7807.74	0.51	7807.86	6.18E-07	7807.86	0.48	0.48	0.045	0.53
H_2O	0	38375.20	38375.20	36045.50	36045.50	36045.50	2.78E-6	36045.50	36014.50	31.03	2.55E-6	2.55E-6	0.16	1706.07
HCL	0	279.60	279.60	279.60	279.60	279.60	9.39E-45	279.60	279.60	5.51E-93	9.18E-45	9.18E-45	0	9.18E-45
EG	0	0	0	4013.35	4013.35	0.0011	4013.35	0.0011	6.53E-38	0.0011	4013.38	4013.38	601.79	931.93
PET	0	0	0	0	0	0	0	0	0	0	0	0	0	10872.20
BHET	0	0	0	0	0	0	0	0	0	0	0	0	2.44	612.28

Table S15 continued

Para.	VAP1	LIQ1	S8	VAP2	LIQ2	VAP3	HVAP3	NH2O	S9	VAP4	PRO-PET1	VAP5	S10	S11
Temp./°C	260.00	260.00	260.00	260.00	260.00	255.32	268.21	100.02	280.00	258.91	258.91	291.94	98.23	93.23
Pres./kPa	810.60	810.60	101.33	101.33	101.33	101.33	111.46	101.33	0.13	0.13	0.13	101.33	101.33	101.33
W-PET	0	0	0	0	0	0	0	0	0	0	0	0	0	0
EGDA	4.40	7.02	7.02	4.80	2.21	9.21	9.21	7.40E-09	2.21	2.21	0.0017	2.21	2.21	2.21
TPA	7.76	1250.86	388.78	7.90	380.87	15.67	15.67	1.64E-43	0.00063	0.00058	4.78E-05	0.00058	0.00058	0.00058
HOAC	0.39	0.14	0.14	0.13	0.013	0.52	0.52	0.47	0.013	0.013	2.22E-06	0.013	0.48	0.48
H_2O	1451.42	254.65	510.36	487.66	22.70	1939.08	1939.08	1938.92	379.76	379.73	0.029	379.73	38333.11	38333.11
HCL	0	0	0	0	0	0	0	0	0	0	0	0	279.60	279.60
EG	381.73	550.20	307.87	220.06	87.82	601.79	601.79	1.87E-09	0	0	0	0	1.87E-09	1.87E-09
PET	1.3E-76	10872.2	12023.6	6.27E-76	12023.6	7.55E-76	7.55E-76	0	12442.00	4.48E-73	12442.00	4.48E-73	4.48E-73	4.48E-73
BHET	0.72	611.56	308.93	1.72	307.21	2.44	2.44	1.57E-83	0.37	0.31	0.068	0.31	0.30	0.30

Table S16 Energy balance of case 2

Equipment	RBATCH1	COOLER1	SEP	PUMP1	RADFRAC1		COOLER2	FLASH1	COOLER3	COOLER4
Cost/kw	-171.96	-9154.79	-2.49	0.34	CON: -6788.45	REB: 10348.50	-894.62	7.99	-17.64	-0.30

Table S16 continued

Equipment	CSTR1	FALSH2	CSTR2	FLASH3	COMP	RPLUG	RADFRAC2		FLASH4	M-COMP		COOLER5
Cost/kw	7868.60	0	774.25	0	20.02	1150.97	CON: -1340.89	REB: 172.54	0	CON: -278.19	REB:274.25	-252.34

Table S17. Utilitiy of case 2

Unit processes used	Type of Utility	Quantity	Function
COOLER1	U-2	12137.90 kg/h	Cool the product and co-produce steam for RADFRAC1
PUMP1	Electricity	0.34 kwh	Increase the pressure of the fluid
RADFRAC1	U-1; U-3	U-1:9431.90 kg/h; U-3:21668.10 kg/h	U-1: Cool the top fraction; U-3: Heat the tower kettle;
COOLER2	U-1	1243.00 kg/h	Cooling
FLAH1	U-3	16.70 kg/h	Heating
COOLER3	U-1	24.50 kg/h	Cooling
COOLER4	U-1	0.40 kg/h	Cooling
CSTR1	Electricity	7868.60 kwh	Heating
CSTR2	Electricity	774.25 kwh	Heating
RPLUG	Electricity	1150.97 kwh	Heating
COMP	Electricity	20.02	Increase the pressure of the fluid
RADFRAC2	U-1; U-3	U-1:1863.00 kg/h; U-3:361.30 kg/h	U-1: Cool the top fraction; U-3: Heat the tower kettle;
MCOMP	U-1; Electricity	U-1:386.50 kg/h Electricity:274.25 kwh	U-1: Compressor interstage cooling; Electricity: Increase the pressure
COOLER5	U-1	350.60 kg/h	Cooling

Table S18. Details of the utilities of case 2

Type of utility used	Initial and final state of utility	
	Initial	Final
U-1	20 ℃;1 atm; liquid phase	100 ℃;1 atm; gaseous phase
U-2	20 ℃;1 atm; liquid phase	250 ℃;39.2 atm; gaseous phase
U-3	250 ℃;39.2 atm; gaseous phase	249 ℃;38.6 atm; liquid phase
Electricity		-

Table S19: Mass balance of case 2

Para.	HOAC	WAS-PET	HOAC1	S2	PRODUCT	LIQUID1	TPA	LIQUID2	EGDA1	OLI-PET1	EGDA2	EGDA3	EGDA4	OLI-PET2	OLI-PET3	EGDA5
Temp./°C	25.00	25.00	118.29	280.00	30.10	30.00	30.00	30.00	215.73	215.73	188.45	224.69	35.00	224.69	35.00	188.71
Pres./kPa	101.33	101.33	102.00	3240.00	105.00	105.00	105.00	121.59	122.27	122.27	101.33	10.00	101.33	10.00	101.33	101.33
W-PET	0	12500.00	0	67.22	67.22	67.22	0	67.22	6.54E-22	67.22	6.54E-22	1.77E-76	1.77E-76	67.22	67.22	6.54E-22
EGDA	0	0	18.75	9473.67	9473.67	9473.67	0	9473.67	9358.23	96.69	9358.23	94.16	94.16	2.53	2.53	9452.39
TPA	0	0	0	10748.20	10748.20	0	10748.20	0	0	0	0	0	0	0	0	0
HOAC	7812.20	0	54505.90	54547.80	54547.80	54547.80	0	54547.80	41.77	0.075	41.77	0.075	0.075	0.00040	0.00040	41.84
H2O	0	0	0	0	0	0	0	0	0	0	0	0	0	0	0	0
PET	0	0	0	0	0	0	0	0	0	0	0	0	0	0	0	0
BAET	0	0	0	0	0	0	0	0	0	0	0	0	0	0	0	0

Table S19 continued

Para.	S3	REGDA	S4	VAP1	LIQ1	S5	VAP2	LIQ2	S6	VAP3	S7	RHOAC	HOAC3	HOAC4	PRO-PET	HOAC5	S8
Temp./°C	115.29	198.60	260.00	251.33	251.33	260.00	260.00	260.00	280.00	251.00	255.22	118.00	264.38	260.18	264.38	118.01	118.01
Pres./kPa	101.33	121.59	810.60	506.63	506.63	101.33	101.33	101.33	0.13	101.33	111.46	101.33	0.13	101.33	0.13	101.33	101.33
W-PET	6.54E-22	0	6.54E-22	0	0	0	0	0	0	0	0	0	0	0	0	0	0
EGDA	9452.39	1294.12	1853.93	777.05	1076.88	750.44	517.07	233.37	1.47E-10	1294.12	1294.12	1.32E-09	1.47E-10	1.47E-10	8.47E-14	1.46E-09	1.46E-09
TPA	10748.20	18.70	1164.31	7.27	1157.04	548.30	11.43	536.86	0.0028	18.70	18.70	2.08E-63	0.0027	0.0027	0.00015	0.0027	0.0027
HOAC	41.84	0.54	5853.81	4453.06	1400.75	1919.13	1744.18	175.95	1552.76	6197.22	6197.22	6196.67	1552.56	1552.56	0.20	7749.24	7749.24
H2O	0	0	0	0	0	0	0	0	0	0	0	0	0	0	0	0	0
PET	0	0	11834.70	1.57E-76	11834.7	12551.9	6.18E-76	12551.9	12491.7	7.75E-76	7.75E-76	0	5.49E-73	5.49E-73	12491.7	5.49E-73	5.49E-73
BAET	0	37.52	886.63	9.52	877.10	576.65	27.99	548.66	1.33	37.52	37.52	1.35E-79	1.31	1.31	0.021	1.31	1.31

Supplementary Figures

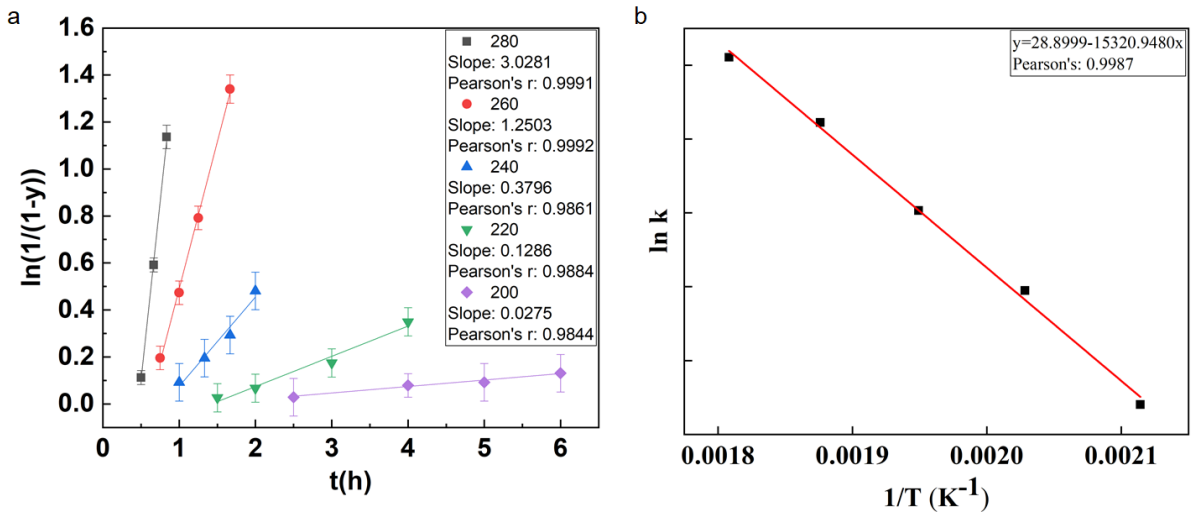

Figure S1. Kinetic data of acetolysis. a, Relationship between ln1/(1–y) and t at different temperatures. **b,** Arrhenius curve of chemical degradation of PET through acetolysis.

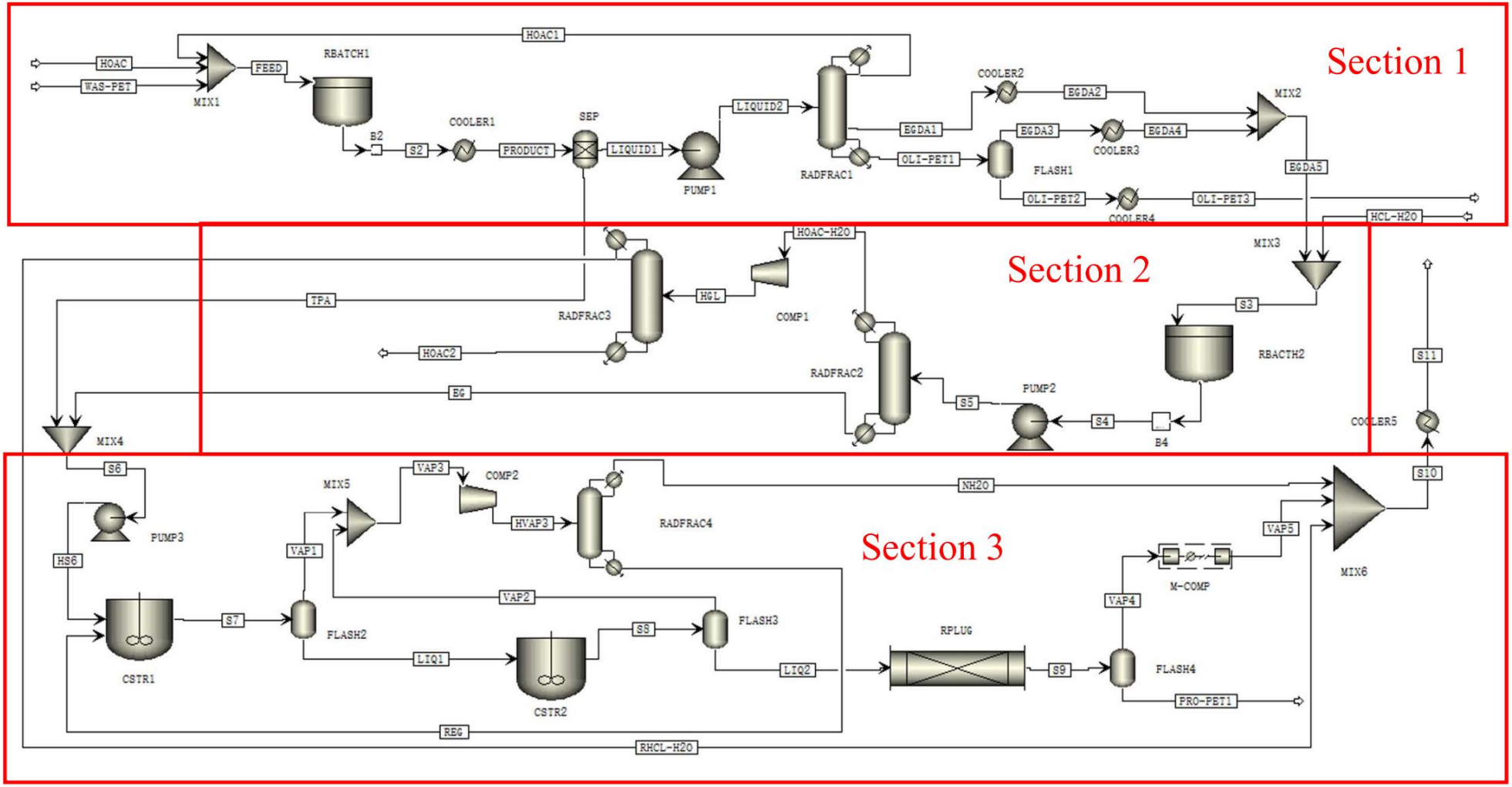

Figure S2. Flowsheet diagram from Aspen model for Case 1

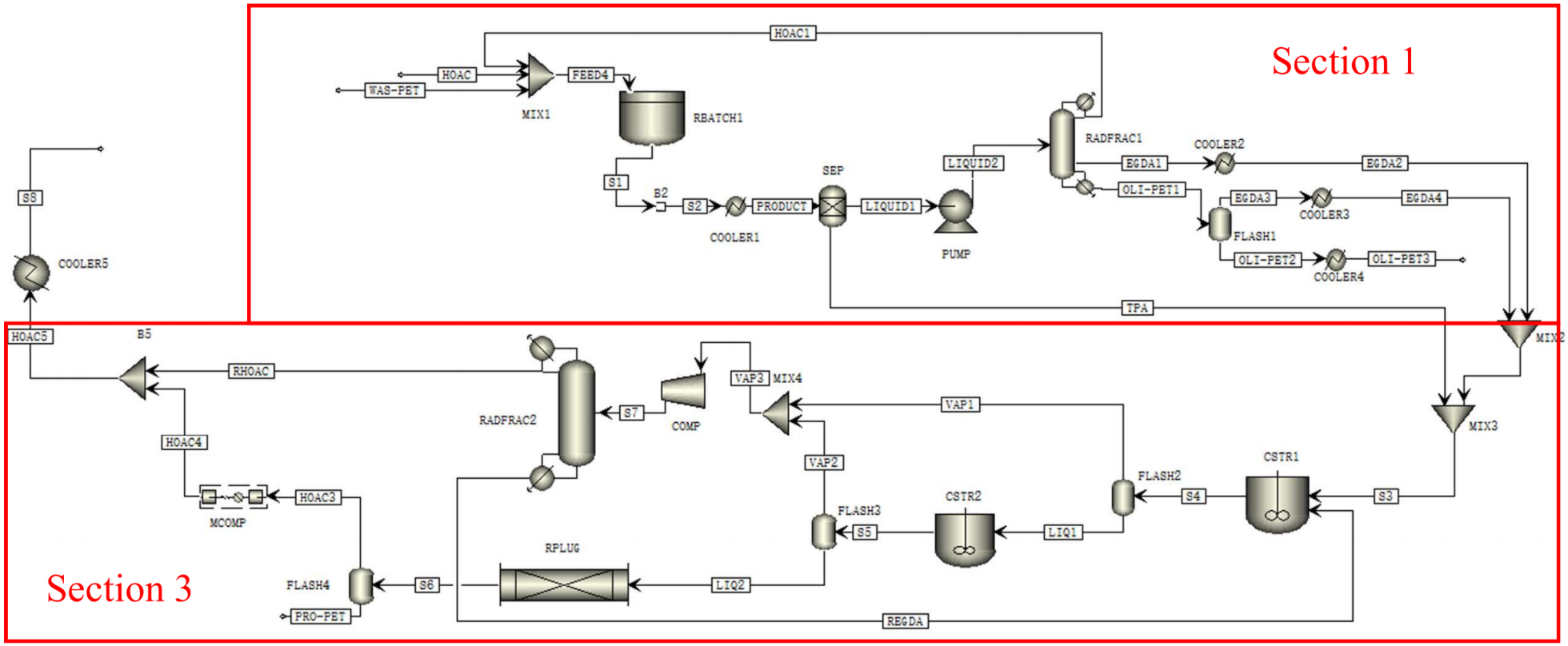

Figure S3. Flowsheet diagram from Aspen model for Case 2

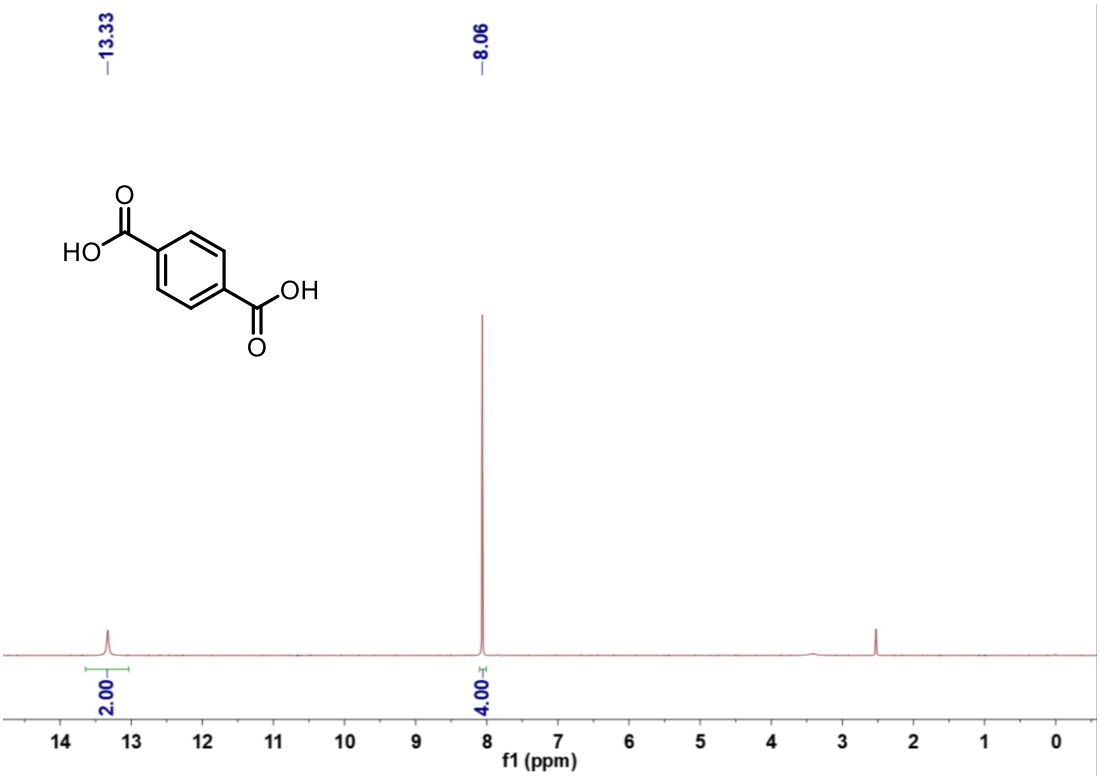

Figure S4. ^{1}H-NMR spectrum of terephthalic acid in DMSO-d_6.

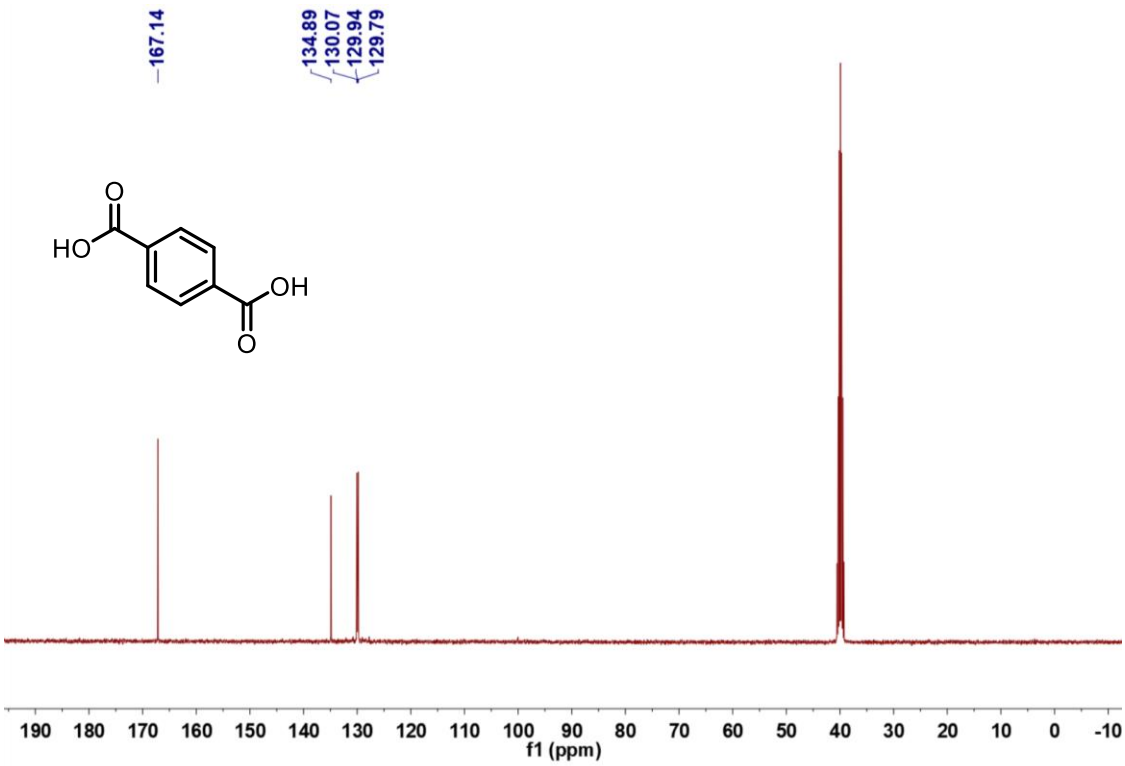

Figure S5. ^{13}C-NMR spectrum of terephthalic acid in DMSO-d_6.

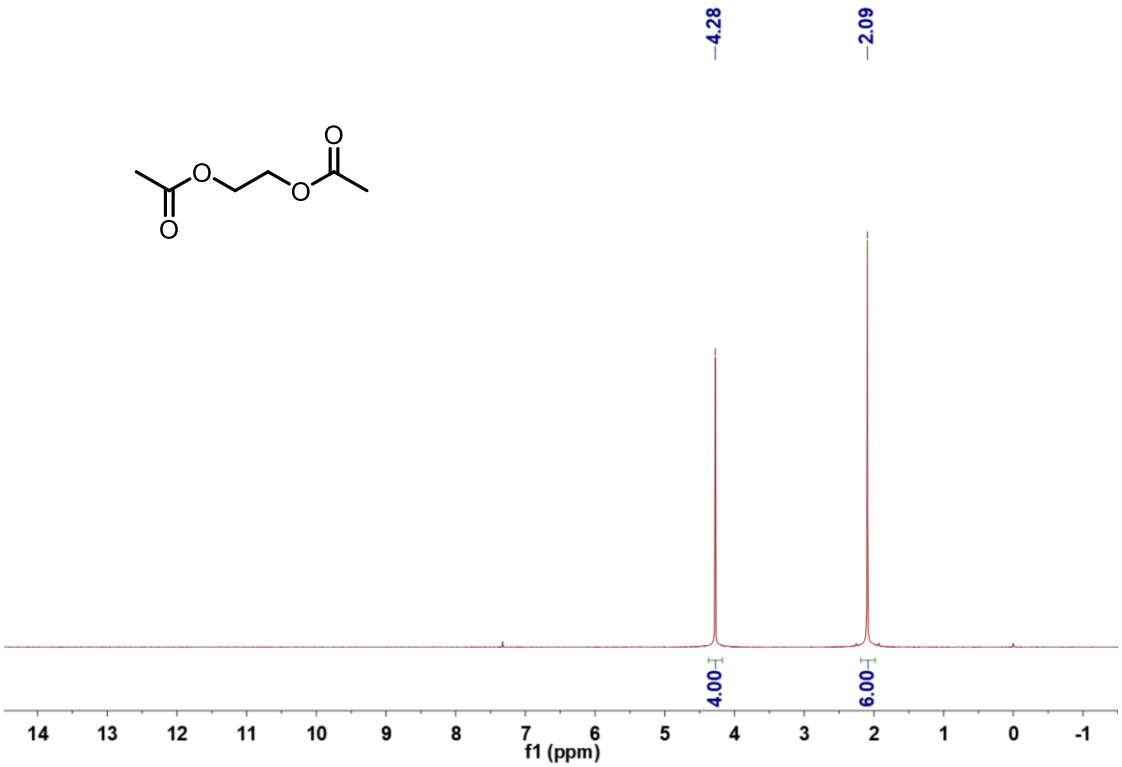

Figure S6. ^{1}H-NMR spectrum of ethylene glycol diacetate in $CDCl_3$.

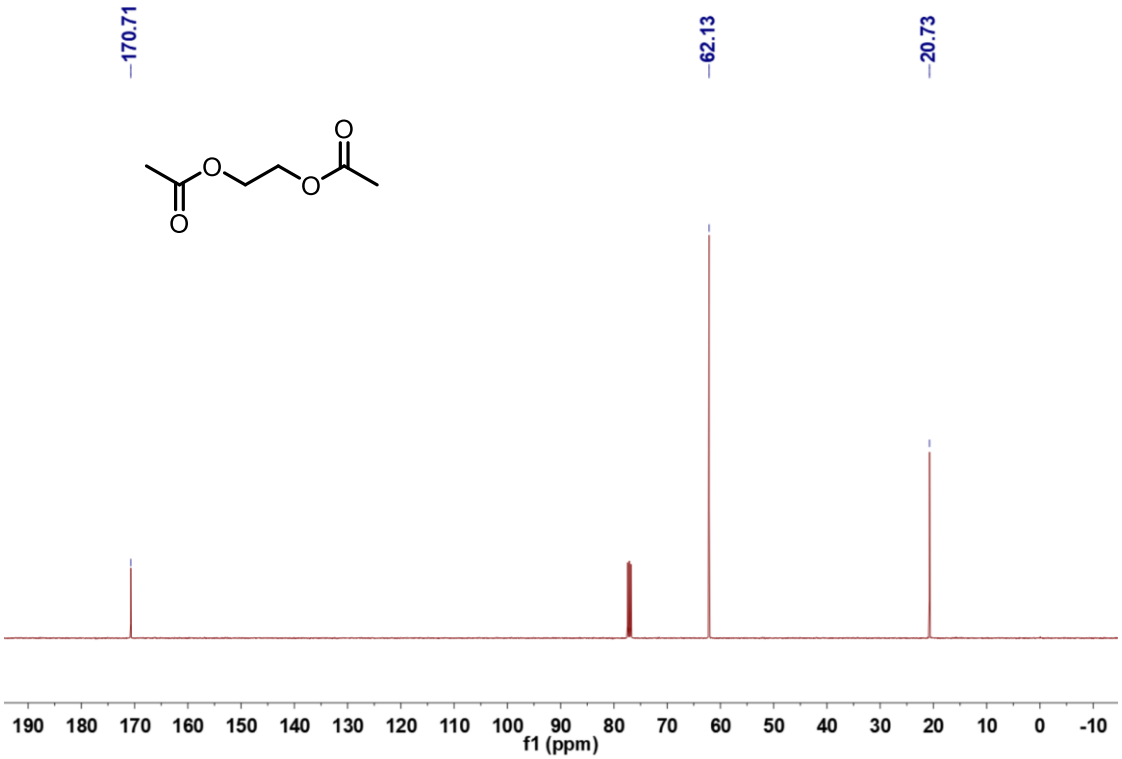

Figure S7. ^{13}C-NMR spectrum of ethylene glycol diacetate in $CDCl_3$.

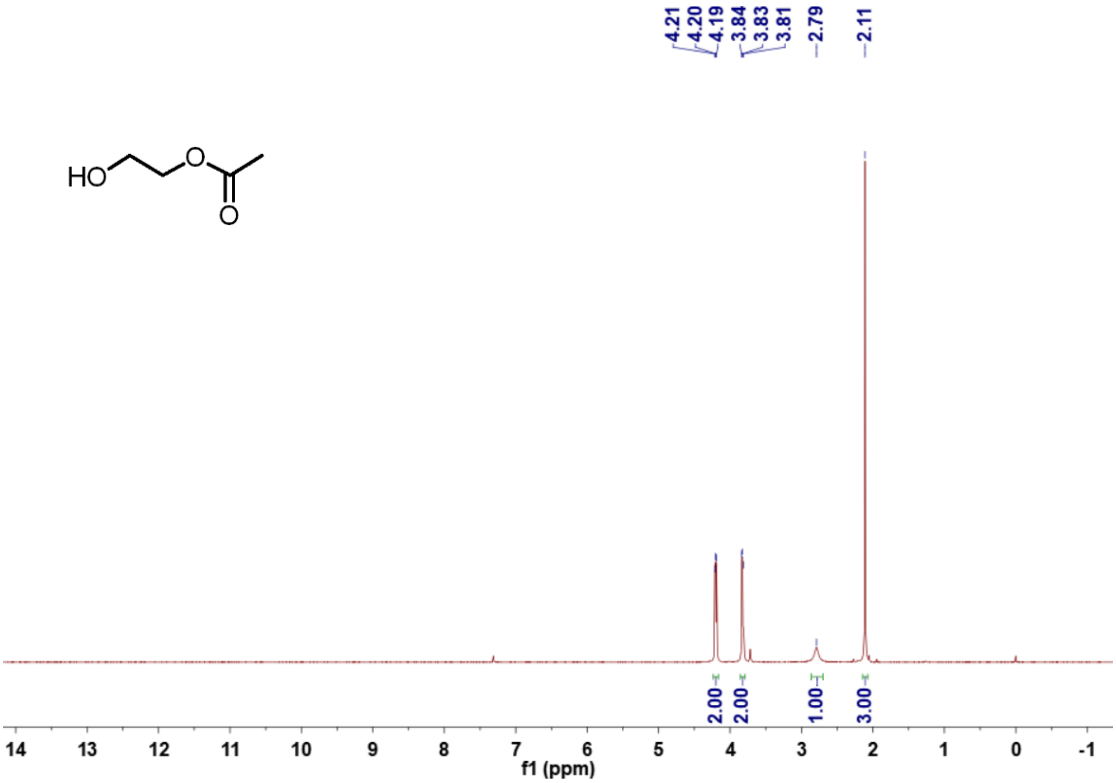

Figure S8. ^{1}H-NMR spectrum of ethylene glycol monoacetate in $CDCl_3$.

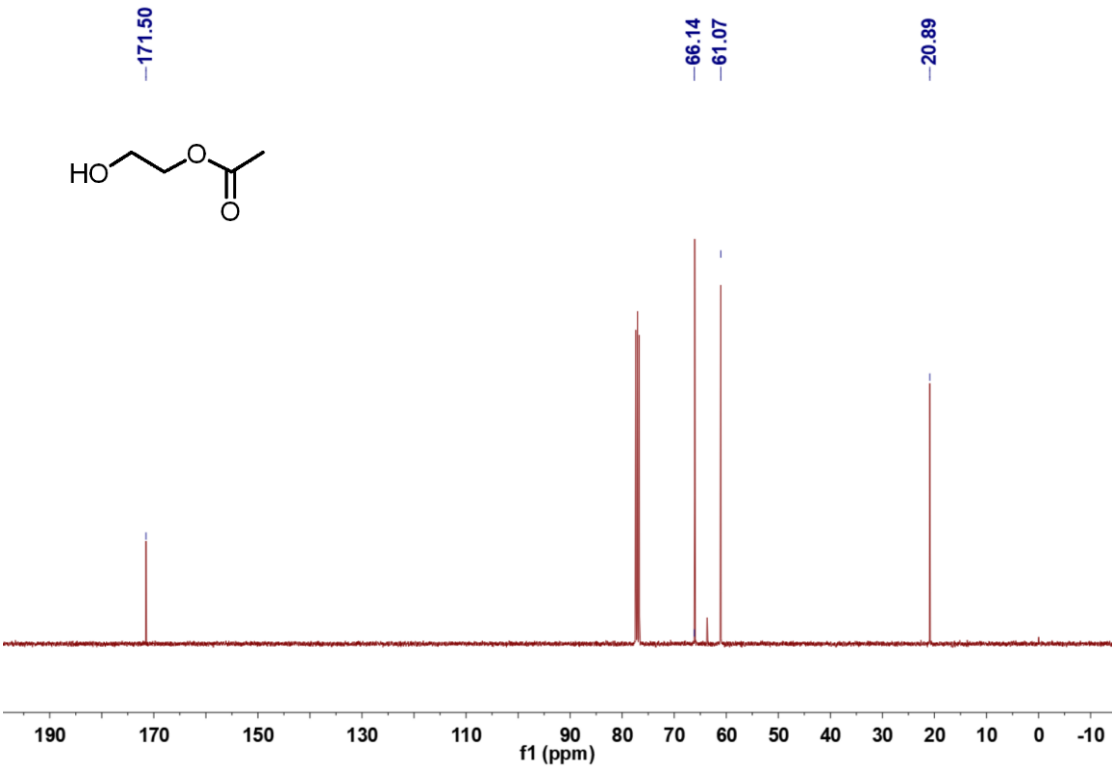

Figure S9. ^{13}C-NMR spectrum of ethylene glycol monoacetate in $CDCl_3$.

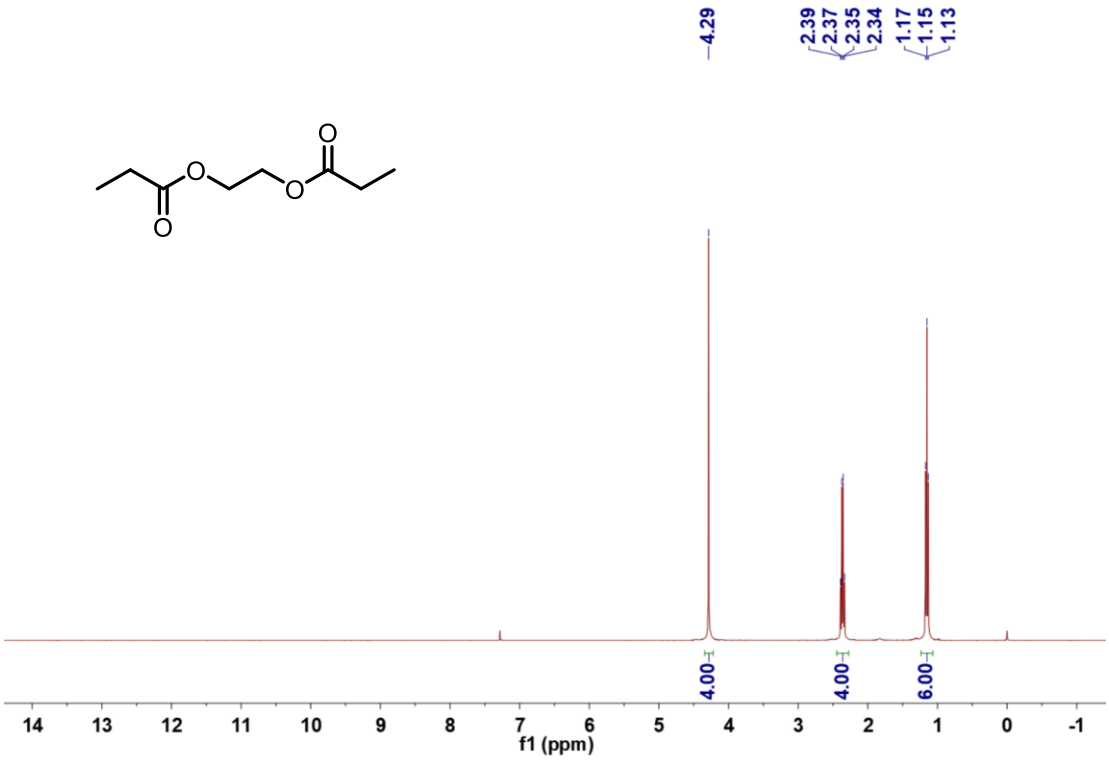

Figure S10. ^{1}H-NMR spectrum of ethylene glycol dipropionate in $CDCl_3$.

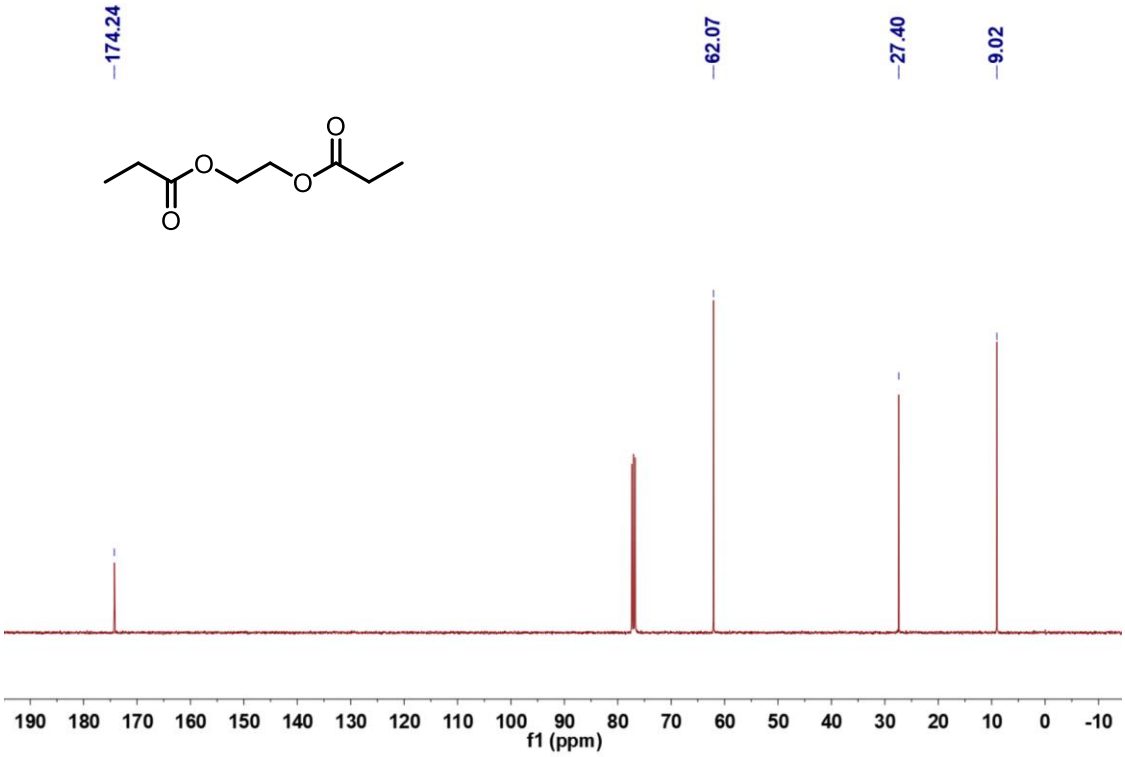

Figure S11. ^{13}C-NMR spectrum of ethylene glycol dipropionate in $CDCl_3$.

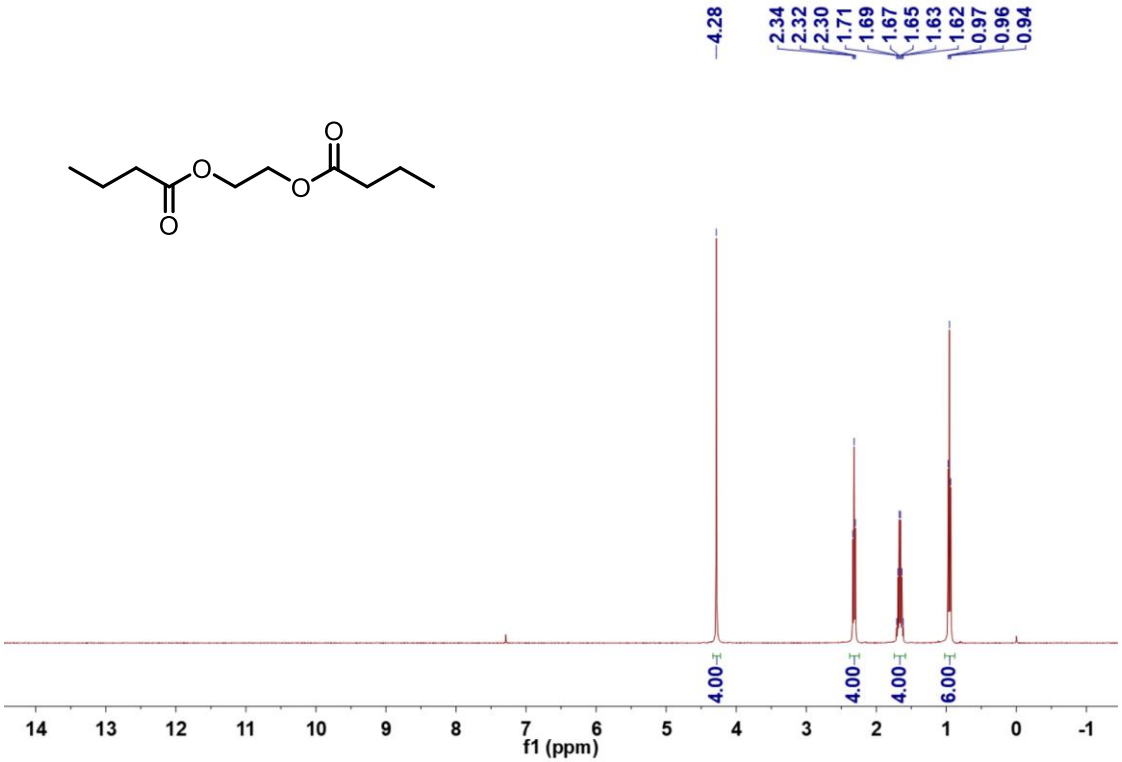

Figure S12. ^{1}H-NMR spectrum of ethylene glycol di-*n*-butyrate in $CDCl_3$.

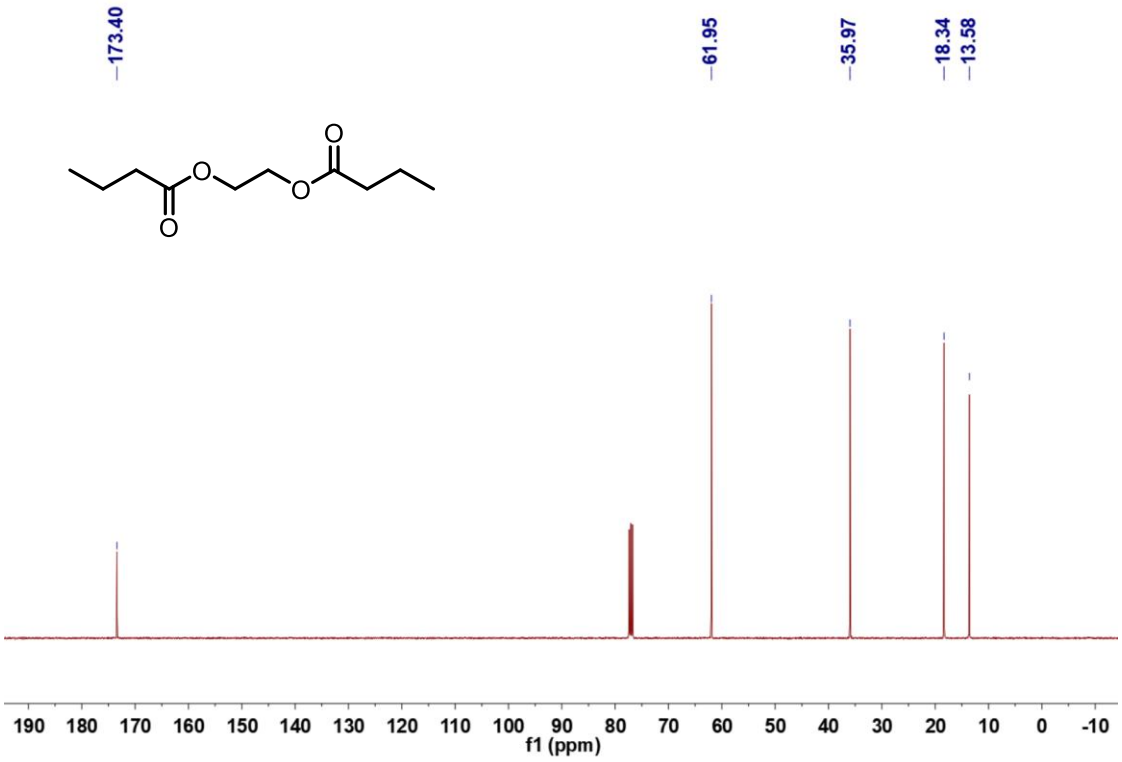

Figure S13. ^{13}C-NMR spectrum of ethylene glycol di-*n*-butyrate in $CDCl_3$.

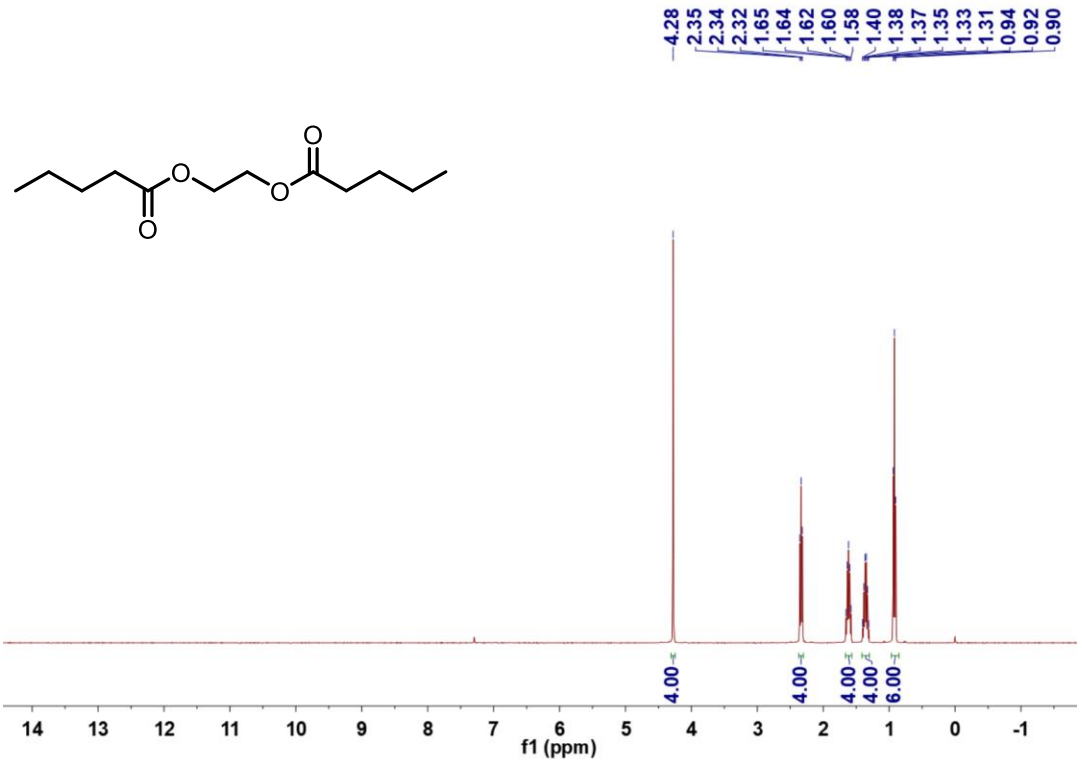

Figure S14. ^{1}H-NMR spectrum of ethylene glycol valproate in $CDCl_3$.

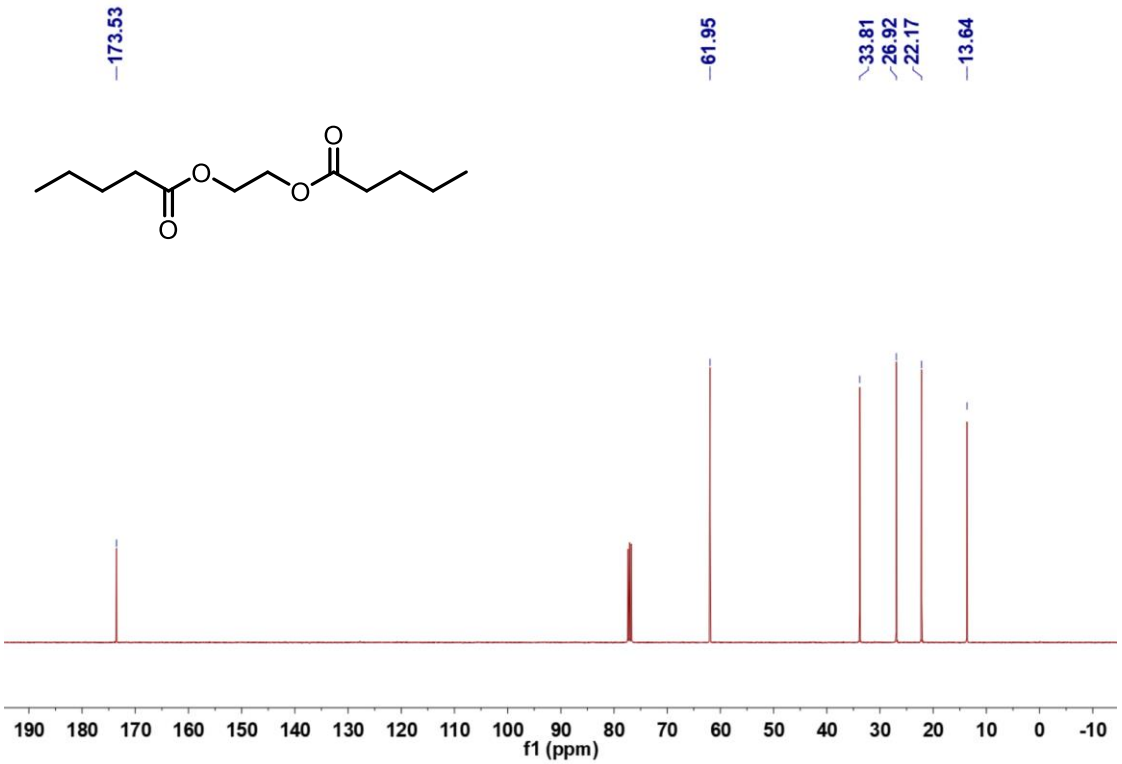

Figure S15. ^{13}C-NMR spectrum of ethylene glycol valproate in $CDCl_3$.

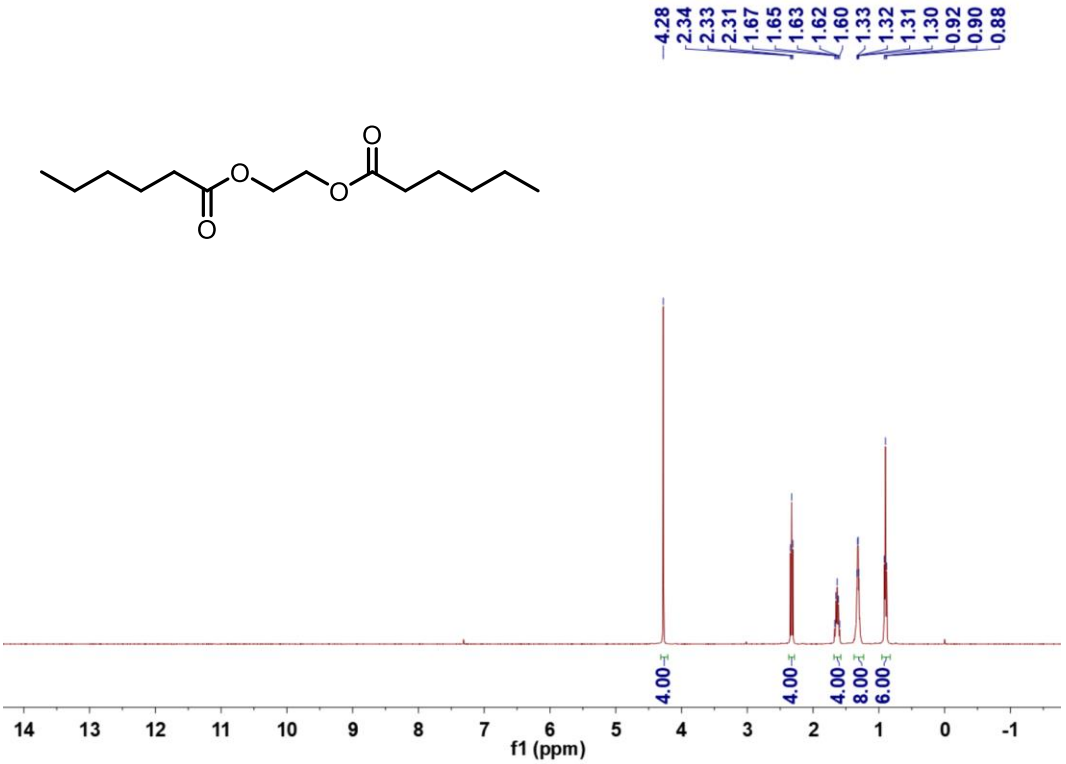

Figure S16. ^{1}H-NMR spectrum of ethylene glycol di-*n*-hexanoate in $CDCl_3$.

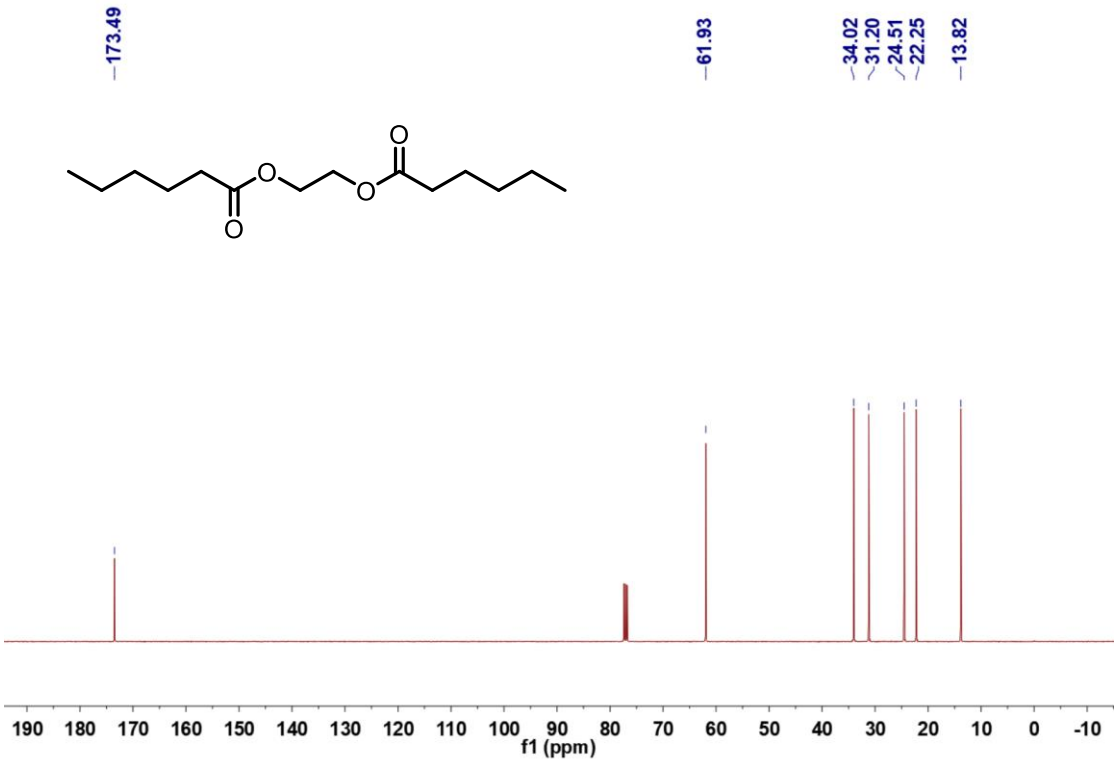

Figure S17. ^{13}C-NMR spectrum of ethylene glycol di-*n*-hexanoate in $CDCl_3$.

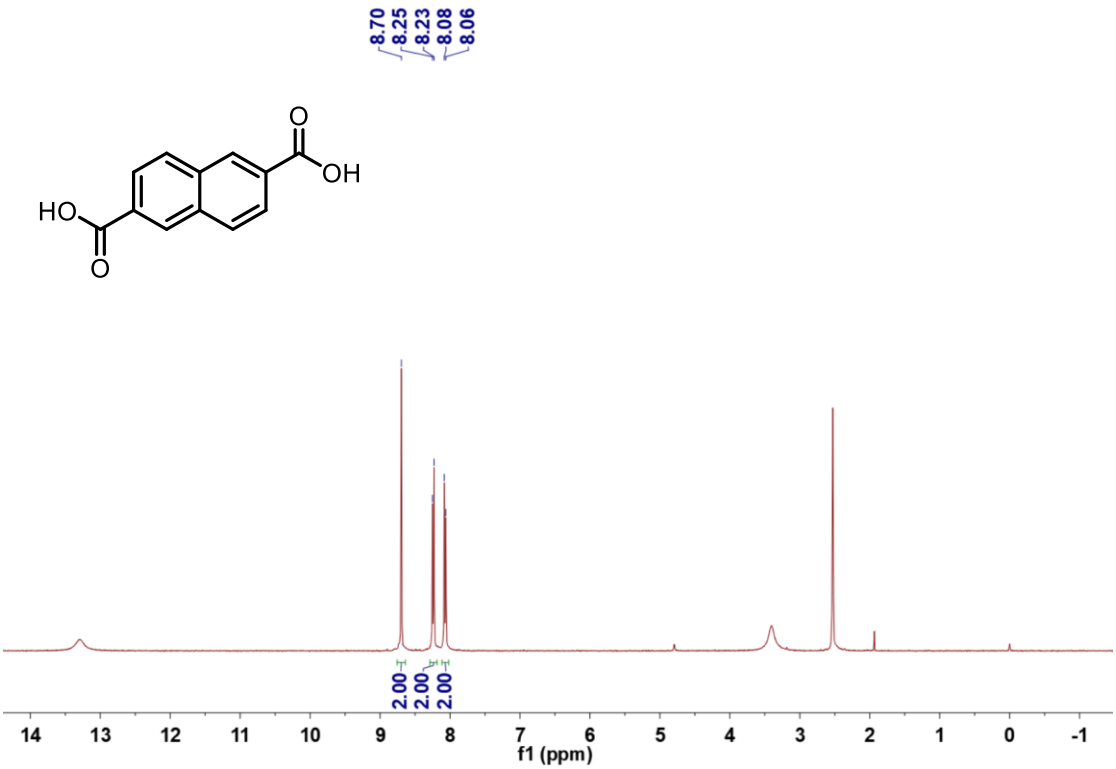

Figure S18. ^{1}H-NMR spectrum of 2,6-naphthalene dicarboxylic acid in DMSO-d_6.

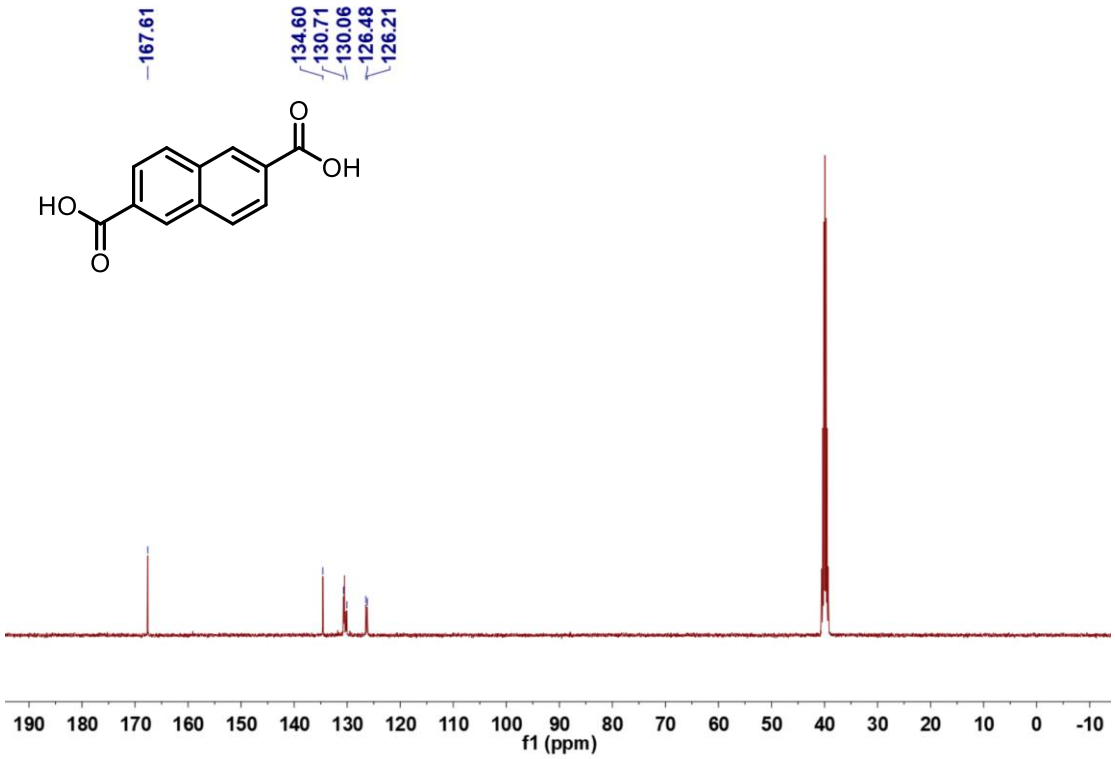

Figure S19. ^{13}C-NMR spectrum of 2,6-naphthalene dicarboxylic acid in DMSO-d_6.

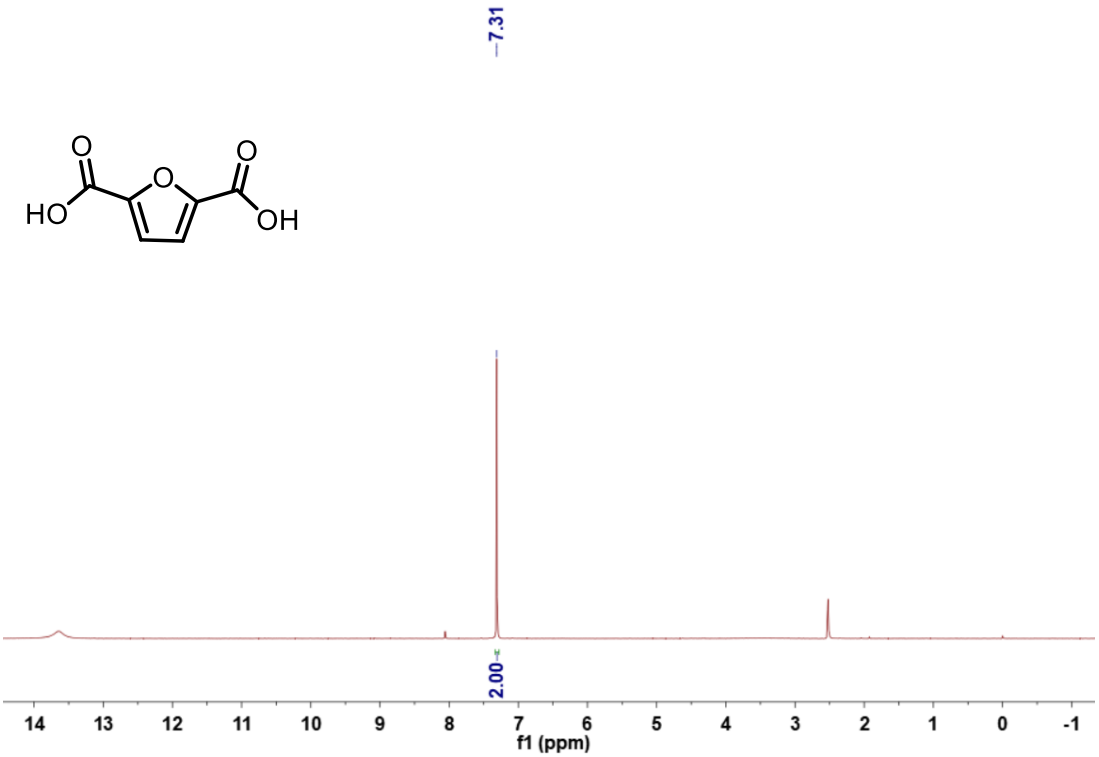

Figure S20. ^{1}H-NMR spectrum of 2,5-furan dicarboxylic acid in DMSO-d_6.

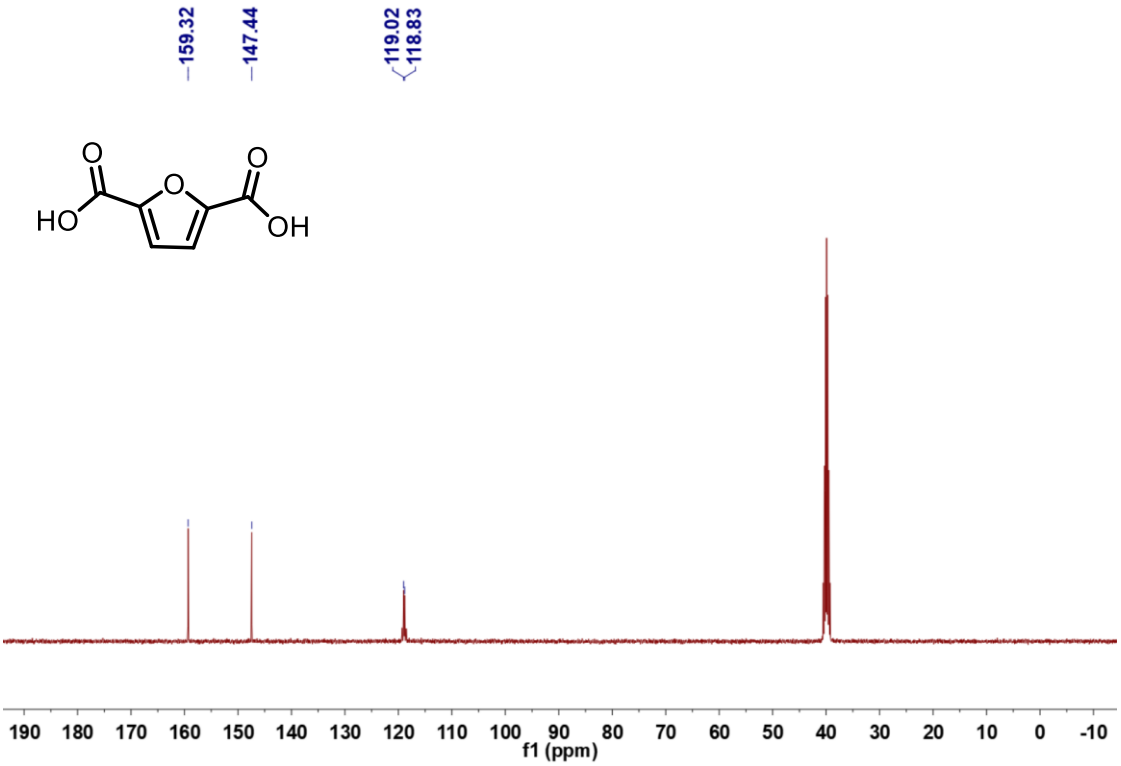

Figure S21. ^{13}C-NMR spectrum of 2,5-furan dicarboxylic acid in DMSO-d_6.

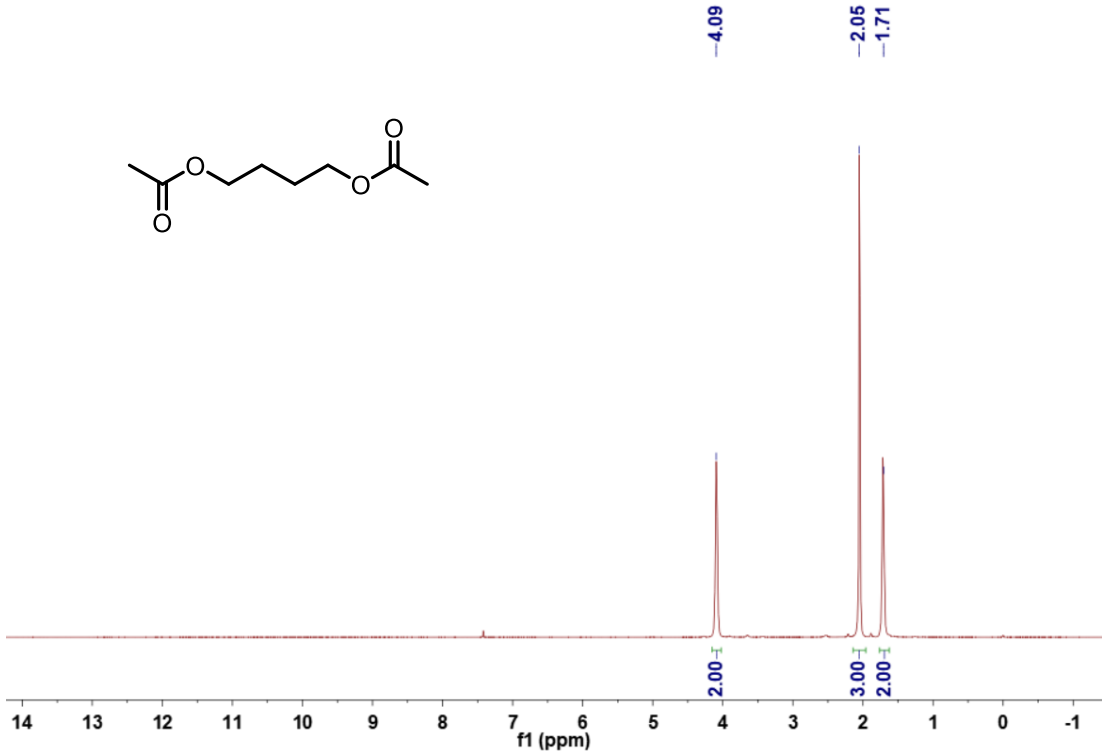

Figure S22. ^{1}H-NMR spectrum of 1,4-diacetoxybutane in $CDCl_3$.

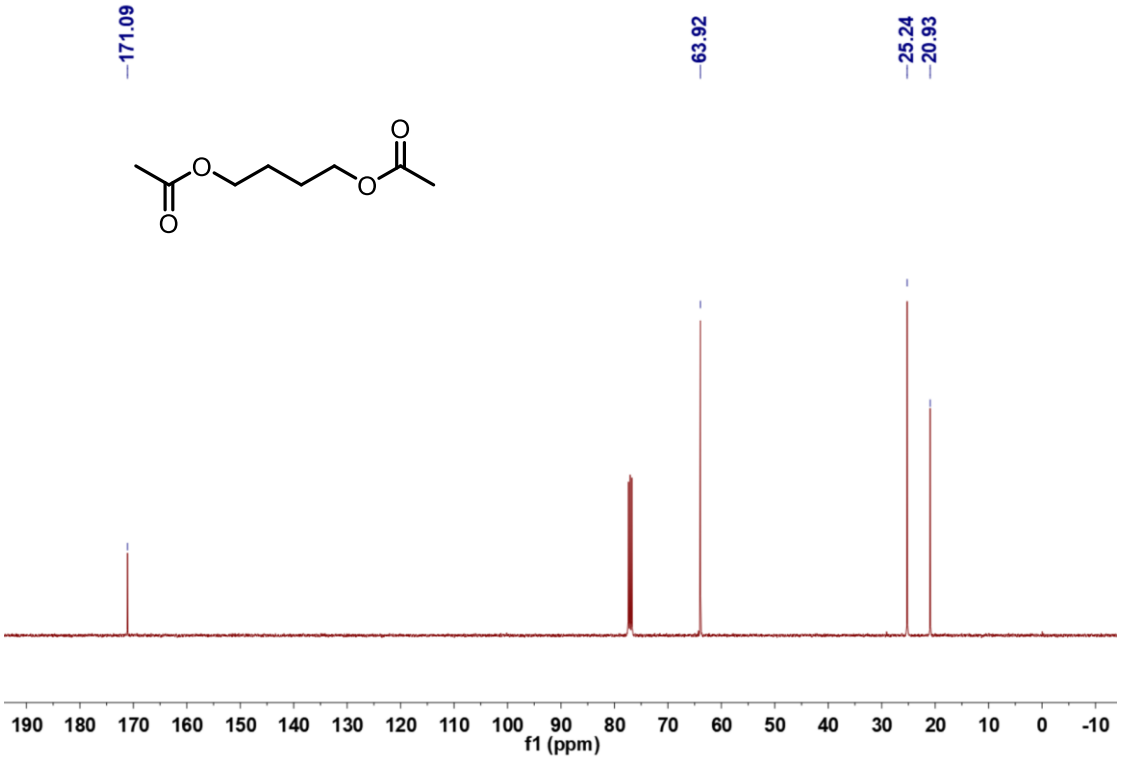

Figure S23. ^{13}C-NMR spectrum of 1,4-diacetoxybutane in $CDCl_3$.

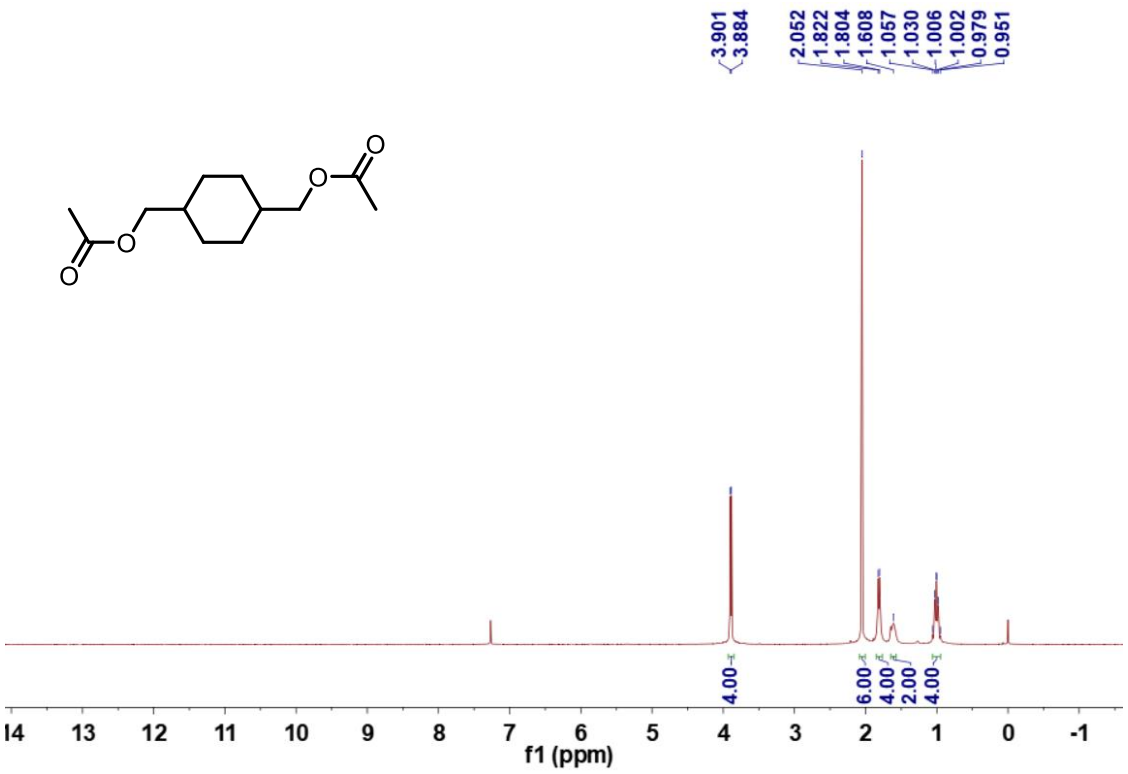

Figure S24. ^{1}H-NMR spectrum of cyclohexane dimethyl diacetate in $CDCl_3$.

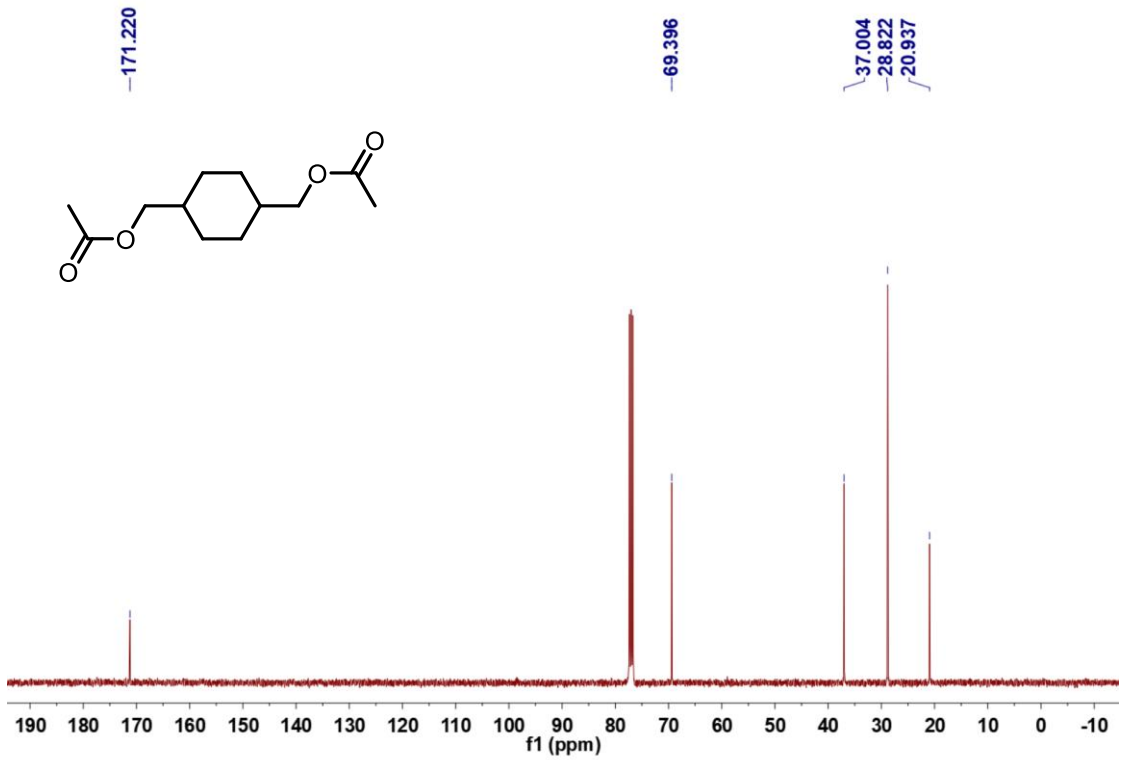

Figure S25. ^{13}C-NMR spectrum of cyclohexane dimethyl diacetate in $CDCl_3$.

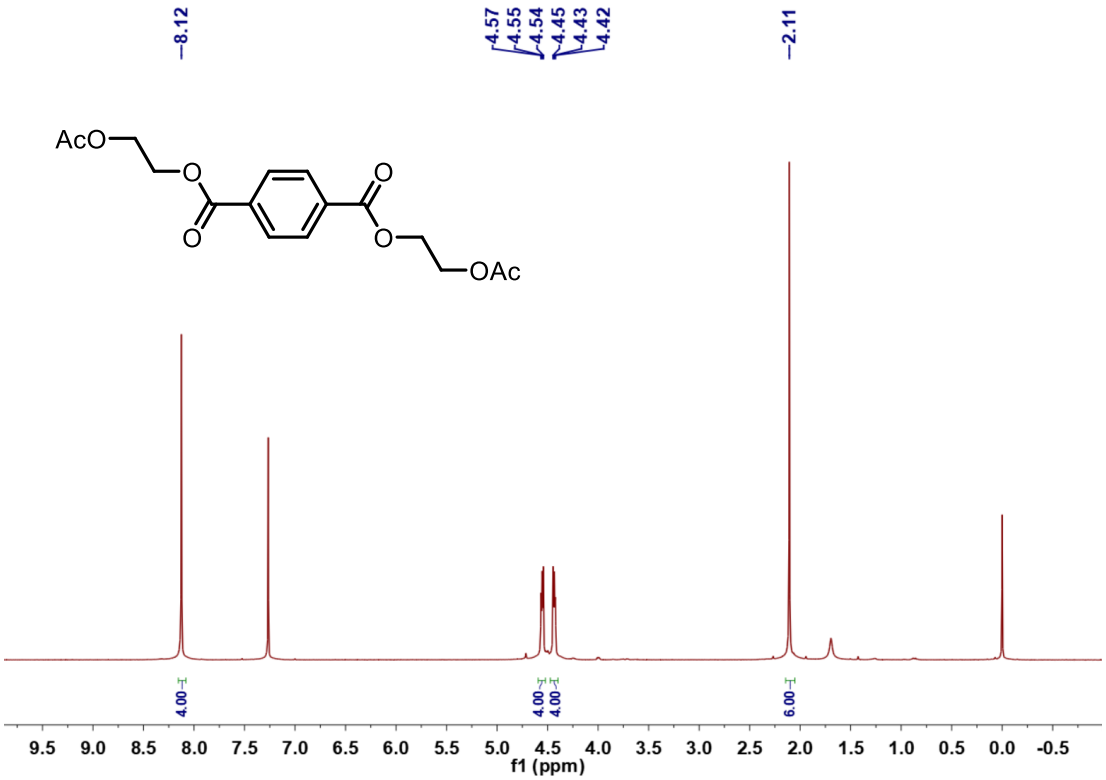

Figure S26. ^{1}H-NMR spectrum of bis(2-acetoxyethyl) terephthalate in $CDCl_3$.

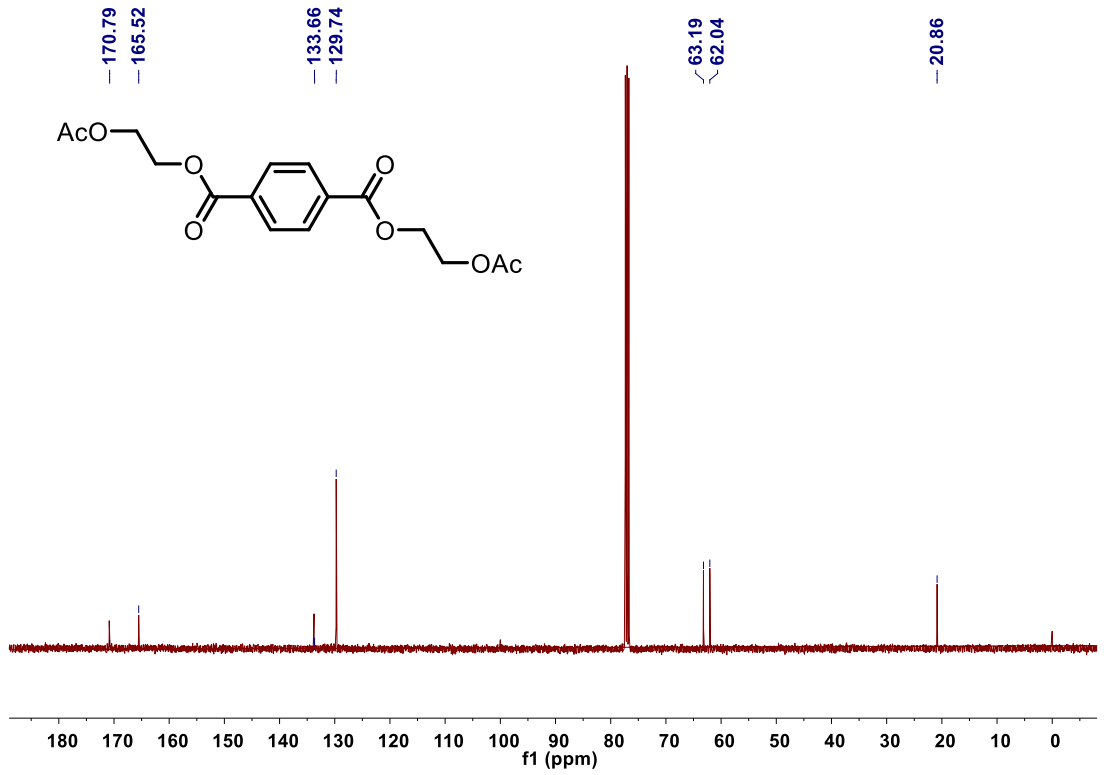

Figure S27. ^{13}C-NMR spectrum of bis(2-acetoxyethyl) terephthalate in $CDCl_3$.

Supplementary Video

The supplementary video shows the depolymerization behavior of waste PET in carboxylic acid. In the video, the valeric acid with low saturated vapor pressure instead of acetic acid was used in the pressure glass tube for depolymerization experiments to observe the reaction process conveniently.

References

1 Kang, M. J., Yu, H. J., Jegal, J., Kim, H. S. & Cha, H. G. Depolymerization of PET into terephthalic acid in neutral media catalyzed by the ZSM-5 acidic catalyst. *Chemical Engineering Journal* **398**, 125655 (2020).

2 Li, X.-K. *et al.* Reaction kinetics and mechanism of catalyzed hydrolysis of waste PET using solid acid catalyst in supercritical CO2. *AIChE Journal* **61**, 200-214 (2015).

3 Yang, W., Liu, R., Li, C., Song, Y. & Hu, C. Hydrolysis of waste polyethylene terephthalate catalyzed by easily recyclable terephthalic acid. *Waste Manag* **135**, 267-274 (2021).

4 Yoshioka, T., Okayama, N. & Okuwaki, A. Kinetics of hydrolysis of PET powder in nitric acid by a modified shrinking-core model. *Industrial & Engineering Chemistry Research* **37**, 336-340 (1998).

5 Ravens, D. A. S. The chemical reactivity of poly(ethylene terephthalate): Heterogeneous hvdrolysis by hydrochloric acid. Polymer **1**, 375-383 (1960).

6 Wang, J. T., Zhou, X. G., Zhao, L., Wang, Y. W., Steady-state simulation of a five-autoclave process polyester industrial plant. *Synthetic Fiber Industry* **35**, 59-63 (2012).

7 Lu, Q. H., Gu, A. J., Zhang, Y. H., & Xie, Z. W., Study and process simulation of polyester polymerization reaction based on Aspen Polymer. *Progress in Chemical Industry* **33**, 1086-1092 (2014).

8 Lu, Q. H., Li, L. J., Zeng, W. B., & Xie, Z. W., Four kettle process modeling for polyester production based on Aspen Polymer. *Synthetic Fiber Industry* **37**, 56-60 (2014).

9 C, K., Y, S. & Liu, A. Step-Growth Polymerization Process Modeling and Product Design. 651-673 (John Wiley & Sons Inc. Press, 2008).

10 Mata-Segreda, J. F. Isergonic relationship in the acid-catalyzed hydrolysis of carboxylic esters with hydrogen-bonding capability. *Journal of Physical Organic Chemistry* **17**, 567-571 (2004).

11 Shen, L., Worrell, E. & Patel, M. K. Open-loop recycling: A LCA case study of PET bottle-to-fibre recycling. Resources, Conservation and Recycling **55**, 34-52 (2010).

12 American Society for Testing and Materials. Determination of 4-carboxybenzaldehyde and p-toluic acidin purified terephthalic acid by reverse phase highperformance liquid chromatography: ASTM D7884-2020. West Conshohocken: ASTM International, 2020.

13 General Administration of Quality Supervision, Inspection and Quarantine of the People's Republic of China, Standardization Administration of the People's Republic of China. Purified terephthalic acid (PTA) for industrial use: GB/T 32685-2016. Beijing: Standards Press of China, 2016.

14 American Society for Testing and Materials. Specification for purified terephthalic acid (PTA): ASTM D7976-2020. West Conshohocken: ASTM International, 2020.

15 Gotze, R., Pivnenko, K., Boldrin, A., Scheutz, C. & Astrup, T. F. Physico-chemical characterisation of material fractions in residual and source-segregated household waste in Denmark. *Waste Manag* **54**, 13-26 (2016).

16 Huggins, M. L. Theory of solutions of high polymers. *Journal of the American Chemical Society* **64**, 1712-1719 (1942).

17 Huggins, M. L. Some properties of solutions of long-chain compounds. *J Phys Chem-Us* **46**, 151-158, doi:DOI 10.1021/j150415a018 (1942).